EXPERIMENTAL EVALUATION OF UWB CHANNEL WITH HUMAN BODY FOR WBAN

PHOUTHONG SOUTHISOMBATH

A THESIS SUBMITTED IN PARTIAL FULLFILLMENT
OF THE REQUIREMENT FOR THE DEGREE OF
MASTER OF ENGINEERING IN COMPUTING IN ENGINEERING SYSTEMS
INTERNATIONAL COLLEGE
KING MONGKUT'S INSTITUTE OF TECHNOLOGY LADKRABANG
ACADEMIC YEAR 2015
KMITL-2015-IC-M-11-01

Thesis Title	EXPERIMENTAL EVALUATION OF UWB CHANNEL WITH HUMAN BODY FOR WBAN
Student's Name	Ms. Phouthong Southisombath
Student's ID	7610018
Degree	Master of Engineering
Program	Computing in Engineering Systems
Year	2015
Thesis advisor	Dr. Sathaporn Promwong

ABSTRACT

An ultra-wideband impulse radio (UWB-IR) technology is excellent contribution for wireless body area network (WBAN) applications due to its low power radiation, robustness against multipath and compact scale. However, it has a problem on distorted waveform through a human body channel. Hence, the objectives of this thesis is to improve the received waveform distortion by introducing matched filter at the receiver side to maximize of signal to noise ratio (SNR). The waveform were analyzed in case of single and double transmission waveform, and channel measurements are performed in frequency domain using a vector network analyzer (VNA) in the frequency range of 3 GHz to 11 GHz with rectangular passband UWB transmitted waveform, which also done in an indoor environment at 3rd floor of UWBIR laboratory building. The double waveform transmission is applied for significantly improving the performances of UWB communication system. On the other hand, this thesis also evaluated and compared the experimental results for the channel transfer function, path loss, received waveform in case of within and without matched filter, power delay profile (PDP), and bit error rate (BER) a performances of single and double waveform transmission model. As considerations, the double waveform transmission can obviously improve performance of UWB transmission waveform for WBAN system.

ACKNOWLEDGEMENTS

This work would not have been possible without the help and support during my completion of this thesis. First and foremost, I would like to express my sincere gratitude to my advisor Dr. Sathaporn Pormwong, Department of Telecommunication Engineering, KMITL for his continues support, his professional guidance, his brilliant comments and his suggestions. For his guidance and advice helped me overcome many technical obstacles which otherwise would take much more effort throughout my master study at King Mongkut's Institute of technology Ladkrabang. The chance that was given to me as one of the UWBIR laboratory member is highly appreciated that I have met friendly people with the greatest manner that I have ever met in the Land of Smiles Country.

I also appreciate to thank my committees for their time to give valuable comments without their suggestions my thesis wouldn't be completed. In addition, many thanks to AUN/Seed-Net JICA project for financial support during my master study at KMITL. Special gratitude and appreciation to KMITL for giving me the great opportunity to do my research study.

I would also like to thank my friends and colleagues all of my sisters and brothers in the UWBIR laboratory, who have accompanied, helps and guidances in everything throughout my master journey and never made things difficult for me. Without their help, advice and encouragement, this thesis would not have happened. And also could not have succeed in my research as well as my life in Thailand. Apart from these, I cannot miss this opportunity to express my appreciation to all of Lao students, Thai students, Cambodia students and Myanmar students at KMITL who always stand by me. I will remember the time we had together and wish them success with everything in their lives.

Last but not least, I would like to thank my family, especially my beloved parents and my brother for their provided unflagging love, encouragement, belief and high expectations. Without my family's constant support and understanding, it would not have been possible for me to achieve my educational goals.

Bangkok, 25 May 2016

Phouthong Southisombath

TABLE OF CONTENTS

TABLE OF CONTENTS (Cont.)

TABLE OF CONTENTS (Cont.)

LIST OF FIGURES

Figures Page

LIST OF FIGURES (Cont.)

LIST OF FIGURES (Cont.)

LIST OF TABLES

LIST OF ABBREVIATIONS

3D	Three Dimensional
ADC	Analog-to-Digital Converter
BAN	Body Area Network
BER	Bit Error Rate
BW	Bandwidth
CEPT	European Conference of Post and Telecommunication
DC	Direct Current
DS-UWB	Direct Sequence Ultra Wideband
DWT	Double Waveform Transmission
EC	European Commission
EFC	Electrical Filed Communication
ETSI	European Telecommunications Standard Institute
EU	European
FCC	Federal Communication Commission
FM-UWB	Wideband Frequency Modulation
HBC	Human Body Communications
HR-WPANs	High Rate Wireless Personal Area Networks
IEEE	Institute of Electrical and Electronics Engineers
ISM	Industrial Scientific and Medical
ITU-R	International Communication Union's Radio Sector
LOS	Line of Sight
LR-WPAN	Low Rate Wireless Personal Area Network
MB-OFDM	Multi-band Orthogonal Frequency Division Multiplexing
MICS	Medical Implanted Communication Service (MICS)
NB	Narrowband
NTIA	National Telecommunications and Information Administration
PDP	Power Delay Profile
PHY	Physical Layer
PSD	Power Spectral Density
QoS	Quality of Service
RF	Radio Frequency
Rx	Receiver
SNR	Signal to Noise Ratio
TG6	Task Group 6
Tx	Transmitter

UWB	Ultra Wideband
UWB-IR	Ultra wideband Impulse Radio
VNA	Vector Network Analyzer
WBAN	Wireless Body Area Network
WPAN	Wireless Personal Area Network
WLAN	Wireless Local Area Network
WMAN	Wireless Metropolitan Area Network
WSN	Wireless Sensor Network
WMTS	Wireless Medical Telemetry Service

CHAPTER 1

INTRODUCTION

1.1 Research Background

Nowadays, wireless communication systems are becoming very popular topic in daily life for short range communications. Moreover, Body area network (BAN) has been developed for monitoring soldiers on the battlefield, managing patients in forward locations in emergency management, elder care and rehabilitation purposes. However, there is an increasing demand for effective communication technologies to support emerging health care delivery systems, wireless body area network (WBAN) for sensing and monitoring of vital signs is the one of most rapid growing wireless communication systems. The requirement have led to increasing research and development activities and promotes new applications for the ambulatory health monitoring of chronic patients and the elderly population, aiming to improve their quality of life in the WBAN applications area for many purposes. Especially WBAN and the Ultra Wideband (UWB) technologies are widely used for a variety of many applications because of its potential in high data rates, low power consumption and low cost [1-2]. Figure 1.1 shows a wireless body network, which consists of radio protocols and standards [3].

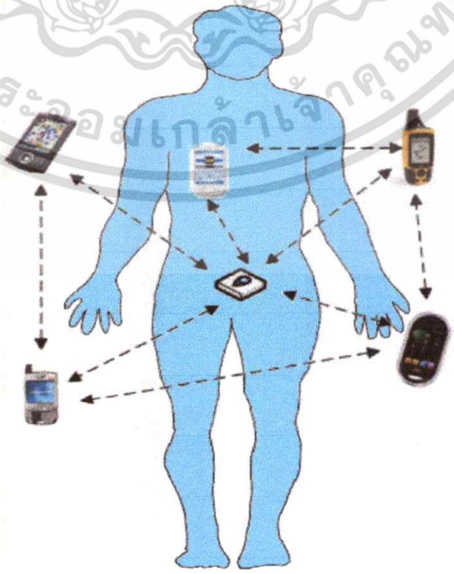

Figure 1.1 WBAN communication systems [3].

1.2 Statement of the Problems

UWB communications systems can be viewed as spread spectrum systems with an extremely large spreading factor [4-5]. Traditionally, UWB radio systems have referred to wireless devices with -10dB fractional bandwidths greater than 25%, or absolute bandwidths greater than 1.5 GHz. This large bandwidth can be achieved by driving an appropriately designed antenna with very short electrical pulses. More recently the Federal Communications Commission (FCC) [6] has defined a UWB device as one that has a fractional bandwidth greater than 20% or that occupies at least 500 MHz of spectrum. Furthermore, the FCC has regulated the spectral shape and maximum power spectral density of a UWB radiation in order to limit the interference with other systems. Also note in part 15 (-41.3 dBm/MHz) still applies.

The history of UWB really started in 1895 with Guglielmo Marconi and his spark-gap transmitter until most RF transceivers switched over to narrowband approaches as a result of Armstrong and hetcrodyne techniques [7]. However, it is interesting to note that modern UWB radio systems started as an offshoot of identifying the transient behavior (impulse response) of microwave circuits [8] and have been around for a long time. Not surprisingly, the early name used by UWB systems based on such transient behaviors is impulse radio [9]. The objective of this study is to investigate the transmission characteristics of UWB impulse radio wave systems by using both analytical and experimental approaches. Antennas that can radiate wide band signals will be manufactured and used in the experiments. Many experiments will be conducted so that the transmission of the antennas can be clearly understood. However, many fundamental issues for UWB waveform still remain largely open. These include waveform design, aspects of channel modelling and indoor propagation, transceiver architectures and waveform distortion [10], as well as overlay issue that include coexistence and sensitivity of UWB systems.

An extension Friis' transmission formula [11] suitable for UWB-HB impulse radio will be derived to include the frequency characteristics of the antennas, the frequency characteristics of free space propagation, and the spectrum of the transmitter signal. A scheme for wideband characterization of the antenna transfer function will be developed while the double transmission antenna will be used to increase the accuracy of the measurements. By using a receiver matched filter which is either the received signal template waveform or an isotropic template waveform, the distortion of the transmitted waveform can be quantified. An experimental scheme including all the above methods will be implemented to find of the UWB-HB transmission gain. UWB antennas will be evaluated and the experimental results will be analyzed to give recommendations for the transmission properties of these types of antennas used in the market. Comparison of the results with the IEEE 802.15.3a will also be made. Lastly, the effects of human body, and shadowing from a person will also be investigated.

1.3 The Objectives and Scope of Thesis

The main objective and scope of thesis is to improve the performance of UWB received waveform on human body by using matched filter. The analysis is based on the extension Friis transmission Formula and presented characteristic of transmission waveform on-body to on-body in wireless communication. The purposes of this thesis have been accomplished and given as below:

1. To study the wireless technology and applications to wireless body area networks.
2. To study and analysis of UWB-HB transmission model as a waveform and double directional waveform of arrival (DDOA) based on the extension Friis's transmission formula and introduce matched filter at receiver side to maximal the SNR.
3. Indoor measurement and modeling of UWB-HB transmission waveform in an indoor environment.
4. To evaluated the UWB-HB transmission waveform in case of double transmission waveform and received waveform within matched filter based on measurement data.

1.4 Organization of the Thesis

This thesis is organized according to each chapter as follows:

Chapter 2 focuses on providing the context for this work in term of wireless communication systems, which forms the basics of WBAN and concentrates on frequency regulations. Furthermore, it also provides a comprehensive overview of UWB-WBAN technologies and their principle components and properties. Including history, regulations, standard and applications of WBAN and UWB technologies are described. This chapter also provide a brief describe the requirements and new challenges of WBAN for heal-care applications.

Chapter 3 provides detail and theory discussion of some parameters used in this thesis such as extension Friis' transmission formula, path loss, power delay profile, received waveform and bit error rate.

Chapter 4 illustrates the performance Evaluation of BAN-UWB Communication System with Double Waveform Transmission is studied in this chapter. The modelling of channel transfer function, some important parameters and equipment are introduced based on the measurement setup. In additions, the measurement model is set at the different positions on human body.

Chapter 5 compares the results of the transfer function based on single and double transmission waveform. Moreover, this work describes the results of magnitude, phase, path loss, power delay profile, received waveform within and without matched filter and bit error rate.

Chapter 6 summarizes all results and provides the future work of this master thesis.

CHAPTER 2

UWB-WBAN TECHNOLOGY

2.1 Introduction

UWB has recently gained a lot of interest for WBAN applications. This chapter presented as well as a brief of overview of the UWB-WBAN for wireless communication systems, which is chosen to be used for short range communication and accommodates appropriate in UWB-WBAN technology. Moreover, Friis' transmission formula is very important for estimating the link budget of UWB transmission channel.

2.2 Wireless Body Area Network (WBAN)

Body Area Network (BAN) has a very short history that is still an emerging technology. In addition, BAN technology emerges as the natural by product of existing sensor network technology and biomedical engineering. The first person is Professor Guang-Zhong Yang who has defined the phrase Body Sensor Network (BSN) with publication of his book Body Sensor Networks in 2006. BSN technology represents the lower bound of power and bandwidth from the BAN use case scenarios. However, BAN technology is quite flexible and there are many potential uses for BAN technology in addition to BSNs. Some of the more common use cases for BAN technology are BSN, Sports and Fitness Monitoring, Wireless Audio, Mobile Device Integration and Personal Video Devices Each of these use cases have unique requirements in terms of bandwidth, latency, power usage, and signal distance. IEEE 802.15 is the working group for Wireless Personal Area Networks (WPAN) [IEEE 802.15] [12-13]. The WPAN working group realized the need for a standard for use with devices inside and around close proximity to the human body. IEEE 802.15 established Task Group 6 to develop the standards for BAN. The BAN task group has drafted a (private) standard that encompasses a large range of possible devices. In this way, the task group has given application and device developers the decision of how to balance data rate and power.

A few years ago, there has been a significant increases WBAN communication systems. WBAN can call BSN is a small scale network device that connects independent node are suitable in the clothes and attached on under skin of a body. Recent technology advance has been developing in sensor and low-power integrated circuit to enable remote monitoring of patient. A typical of WBAN consist of a number of smaller size nodes, lightweight, low-power sensing devices and less space covered and applied for many activities function. WBANs typically use a conventional star topology as shown in figure 2.1. Which nodes acquire, process and transmit information to the central hub that would be included in a smartphone for a typical laboratory health monitoring application. These networks are composed by wireless sensor or actuator nodes used for measuring physiological variables (e.g., glucose level in blood or body temperature).

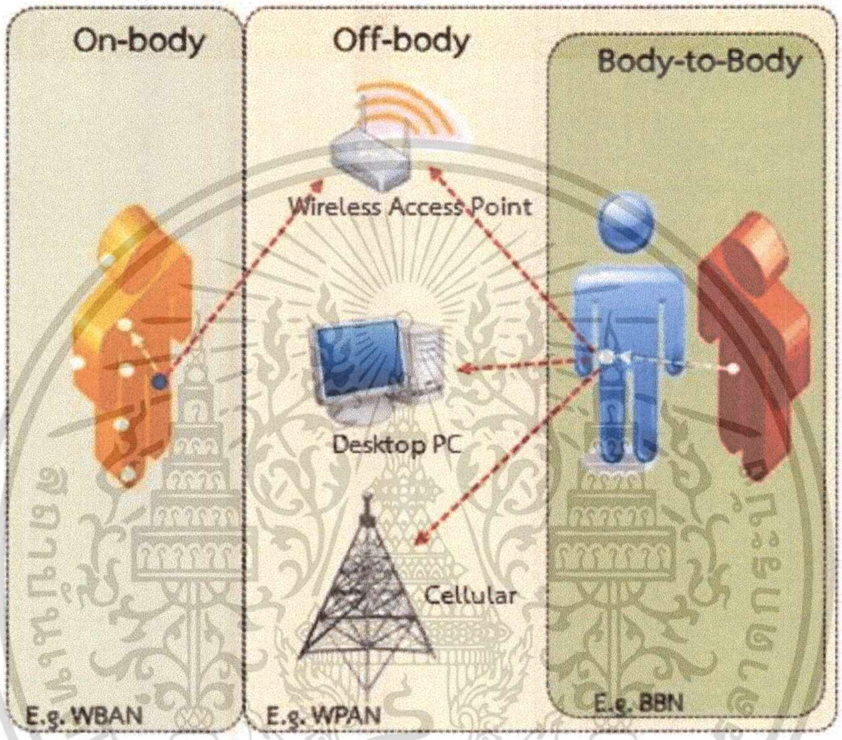

Figure 2.1 Wireless UWB-HB communication network [13].

In general, IEEE 802.15 is the working group for Wireless Personal Area Networks (WPAN). The WPAN working group realized the need for a standard for use with devices inside and around close proximity to the human body [13-14]. IEEE was requested to standardize the Body Area Network. IEEE 802.15 task group 6 (TG6) was set up to develop an IEEE international standard for BAN in January 2008. IEEE 802.15 established Task Group 6 is developing communication standards for BAN as a system optimized for low power devices and operation in, on around the human body to serve a variety of applications including medical, electronics, consumer, personal entertainment and others. The BAN task group has identified four distinct communication scenarios. By the way, the task group 6 has given WBAN standard as shown in table 2.1.

Table 2.1 Standard of IEEE.802.15.6 [14]

Regulation	Values
Distance	below 3m
Power	Less than 25 W
Bit rate	10 Kbps to 5 Mbps
Connection model	Star

2.3 Regulation of WBAN

The worldwide available frequency band for WBAN, it is desirable to designate a worldwide frequency band to support for mobility and designate frequency bands to WBAN with large available bandwidth. Moreover, WBAN may use spectrum with high user density as shown in figure 2.2.

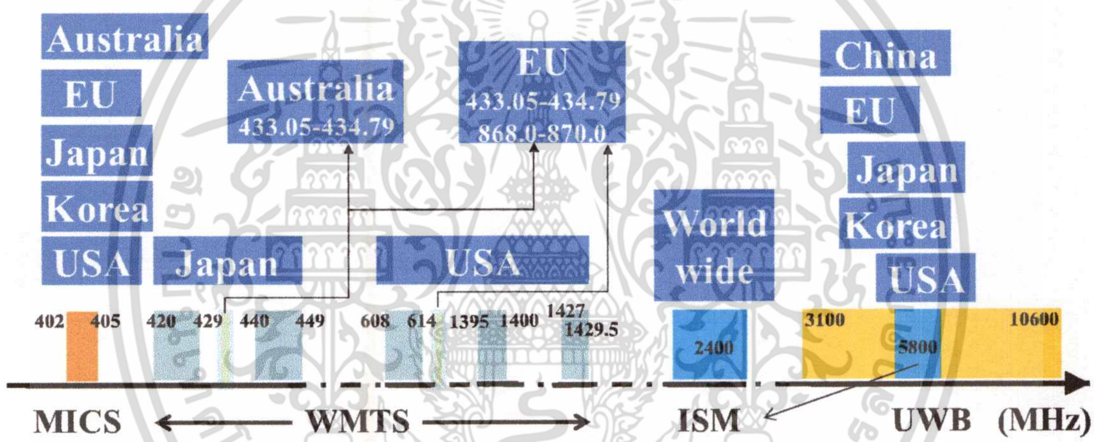

Figure 2.2 Frequency spectrums for WBAN [14].

2.3.1 Medical Implanted Communication Service (MICS)

In 1998, the International Telecommunication Union's Radio Sector (ITU-R) assigned in the band of 402-405 MHz for medical implant communication [15]. Due to this band is widely used in the same worldwide. Moreover, the requirement of devices has a compatible the EIRP is limited to -16 dBm in the bandwidth of 300 KHz. In order to support the simultaneous operation of multiple devices and avoid interferers in the same area, ITU-R recommended a total required bandwidth of 3 GHz to support 10 channels.

2.3.2 Industrial Scientific and Medical (ISM)

The ISM band are internationally band reserved frequency spectrums to be used for ISM band purposes. Due to the radio devices using ISM band are generally allowed for unlicensed operation, ISM band can also be regarded as one of the frequency candidates for WBAN. International frequency allocation for ISM band by ITU radio are contained in the radio regulation (RR) Nos. 5.138, 5.150 and 5.280 [16]. The frequency band that are most suited for WBAN at ISM bands include 433.05-434.79 MHz, 902-928 MHz, and 2400-2500 MHz.

2.3.3 Wireless Medical Telemetry Service (WMTS)

In 2000, Wireless Medical Telemetry Service (WMTS) is a radio communication system. It was available in the USA by the FCC for ambulatory monitoring of a patient's health and gives greater mobility than solutions. The bands defined the frequency ranges are 608-614, 1395-1400 and 1427-1432 MHZ.

2.3.4 Ultra-Wideband (UWB)

UWB system operate at very low radiation power density level by employing very narrow pulse resulting in very large bandwidth. In 2002, the FCC opened a large band from 3.1 GHz to 10.6 GHz [16] with different power levels for UWB. In March of 2004, the European Commission issued a mandate to CEPT to establish a task group on UWB usage. Ultra-wideband has recently become for many years ago and apply for radar, sensing, military communications and niche applications in broadband wireless technology. The UWB is a one of the key emerging technologies that provided for short range and low power radio communication systems with a small devices to medium from factor an indoor application. Several proposals exit for UWB solutions. The performance of investigations have been carried out in BAN technology. The UWB uses an extremely large bandwidth of RF spectrum for transmitting the data with very short pulses and power spectral density (PSD) in the range of ultra wide frequency spectrum instead of using narrow carrier frequency in traditional RF technologies. Moreover, The UWB radio channel bandwidth for WPANs is specified the cover frequencies ranging from 3.1GHz to 10.6 GHz and does not over exceed -41.3dBm/MHz [8]

The United States FCC use the following 2 parts requirement to identify UWB emission which measured at -10 dB factional bandwidth greater than 0.2 or -10 dB bandwidth equal to or greater than 500 MHz [9]. The factional bandwidth is based on the frequency limits of the emission bandwidth using the formula are define as:

$$f_{\mathrm{b}} = f_{\mathrm{H}} - f_{\mathrm{L}} \tag{2.1}$$

$$B_{\mathrm{f}} = 2\frac{f_{\mathrm{H}} - f_{\mathrm{L}}}{f_{\mathrm{H}} + f_{\mathrm{L}}} \tag{2.2}$$

Where f_{H} is the highest frequency and f_{L} is the lowest frequency.

Ultra-wideband is a technology for transmitting information spread over a large bandwidth which measured at -10 dB. The FCC in the United States allocated a factional bandwidth greater than 0.2 and having the occupies bandwidth below the peak emission is 500 MHz. or The UWB transmitter sends a pulse with a channel bandwidth of this wide and the receiver collects the power of the received signal for rebuilding the pulse. Moreover, the spectral density level of UWB signal may be below the noise level of receiver for other systems, UWB devices can operate using spectrum occupied by existing radio services without causing interference, thereby permitting scarce spectrum resources to be used more efficiently [16]. The UWB use an extremely wideband of RF spectrum to transmit the data with very short pulses and PSD in the range of ultra-wide frequency spectrum instead of using narrow carrier frequency in traditional RF technologies. The UWB spectrum is shown in figure 2.3.

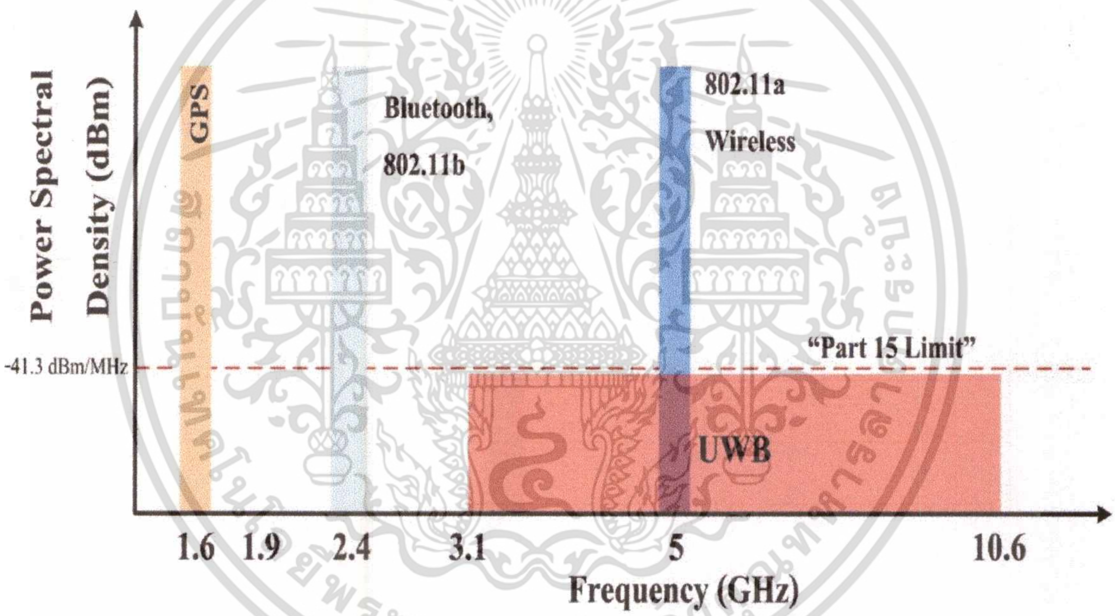

Figure 2.3 Comparison between UWB and other wireless technologies [16].

2.4 Requirement of BAN Technology

BAN has the following significant requirement, these are usually a set of limits or thresholds on the system parameters. For example, an upper limit on the maximum body temperature (system parameter) ensures safety. Similarly, the IEEE 802.15.6 task group on application requirements [18] we can extract the Data rates can not defined the time draft for standard [19].however, the several applications need specific data rates from the technical requirements [10] has support the data rate up to 10 Mbps when using UWB. The security is also mention that will be required for the transport of sensitive data and access to it within base station. For BAN sustainability are to ensure that at least a given number of nodes (system parameter) can be operated using available power from different energy resources.

2.5 Standard and Applications of WBAN

2.5.1 IEEE 802.15.6

Among the many wireless communication standard activities worldwide, the IEEE 802.11 and IEEE 802.15 family of standards have the largest impact on the wireless today. In February 2012, IEEE 802 has established a Task Group called IEEE 802.15.6 standard is a new standard for WBAN [20]. Which aims to provide short range communication (i.e. human range), low power and high reliable for wireless communication.

BAN is defines as a communication which is a small scaled network that operates inside a body. The task group 6 will provide an international standard for highly reliable wireless communication and a short range low power for using in closed vicinity of the human body and it also has optimized low power constraint in-body/on-body nodes to support a variety of medical and non-medical applications [21-23]. Which is used for existing industrial scientific medical (ISM) bands. Support for security, low power devices, quality of service (QoS), data rate up to 10 Mbps is required while simultaneously complying with strict non-interference guidelines where needed and can be offer to satisfy an evolutionary set of entertainment and healthcare services.

2.5.2 Application of WBAN

The WBAN application consists of wearable and implantable sensor nodes that offers many promising applications are not only limited to health care application but it also has non-medical application [23] as entertainment, military, security and sport as shown in figure 2.4 WBAN is mainly except for medical and healthcare monitoring are the one of targeted of WBAN application, assistance to people with disabilities and much more closely patient suffering with chronic diseases such as heart attack, asthmas and diabetes.

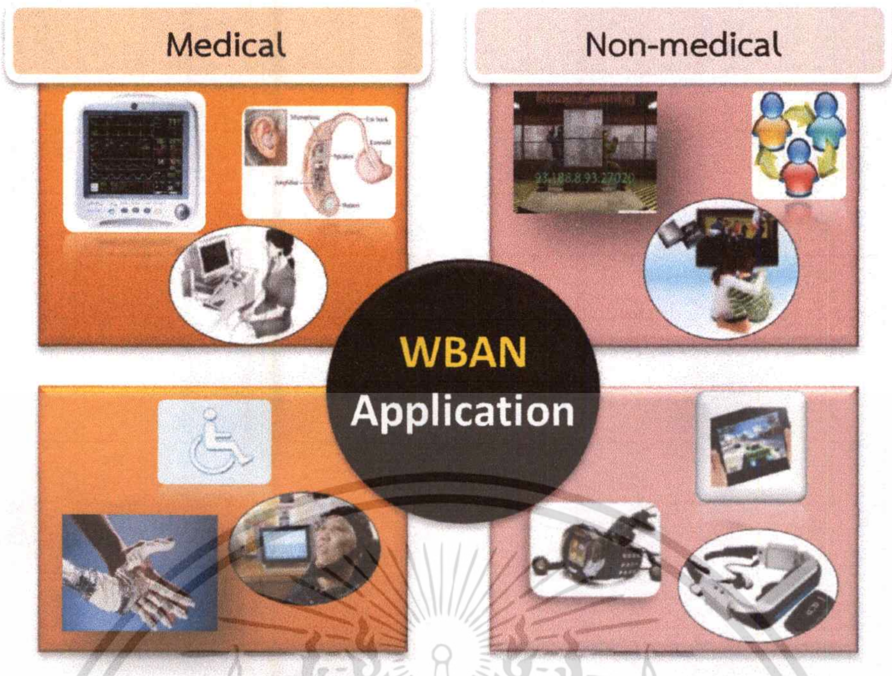

Figure 2.4 WBAN applications [23].

2.6 Physical Layer of BAN Technology

The current IEEE 802.15.6 standard was completed in May, 2010 and supported three mainly different PHY layers of BAN. The IEEE 802.15.6 structure Included Narrowband (NB), UWB, and Human Body Communications (HBC) layers are summarized and shown in figure 2.5.

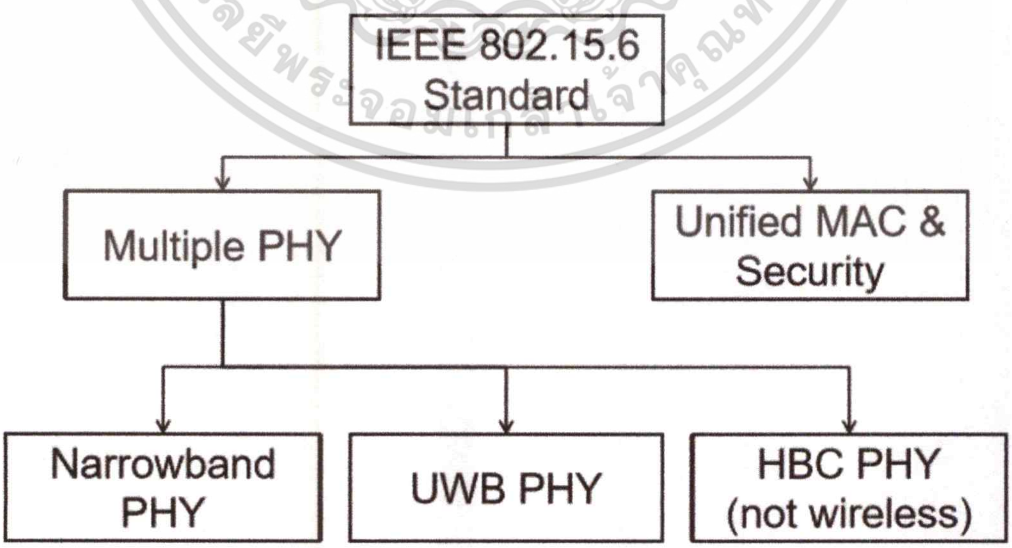

Figure 2.5 Structure of IEEE 802.15.6 standard [19].

2.6.1 Narrow Band (NB)

NB PHY is aimed at communication with the wearable nodes on body and the implantation nodes in body that is an optional layer specified by IEEE 802.15.6 It functions mainly provided in three aspects as following: activation and deactivation of the radio transceiver, clear channel assessment within the current channel and data transmission and reception.

2.6.2 Ultra Wideband (UWB)

The UWB PHY design is not only to improve the robustness of the WBAN, but also provides opportunities for implementation of high performance, low complexity and low power consumption operation. There are two different types of UWB technologies included in the UWB PHY. Namely, impulse radio UWB (IR-UWB) and wideband frequency modulation (FM-UWB). The specification defines two modes of operation: default mode and high quality of service (QoS) mode.

2.6.3 Human Body Communication (HBC)

HBC in some early literature is called Electric Field Communication (EFC), for that EFC is the basic of physical realization. Its transmitter is implemented with only digital circuits and needs one electrode, instead of antenna. The realization of the receiver needs none RF modules, which makes equipment easy to carry and power is very low.

2.7 UWB Regulation

UWB regulation has been opened the door without licenses in February 2002 by FCC as an outcome of deliberation in connection with the National Telecommunications and Information Administration (NTIA) [24].

2.7.1 Regulation in USA

In 1998, the FCC in USA has set out such a mark to regulate UWB technology under the FCC part 15 regulation limitations and allow to use unlicensed of UWB communication [17]. The FCC approved the deployment of UWB frequency range from 3.1 to 10.6 GHz band. The USA spectral mark for indoor and outdoor applications specified by FCC is shown in figure 2.6 and table 2.2.

Table 2.2 FCC limits in USA for indoor and outdoor communication applications [24].

Frequency Ranges (MHz)	Indoor EIRP in dBm	Outdoor EIRP in dBm
960-1601	-75.3	-75.3
1610-1990	-53.3	-63.3
1990-3100	-51.3	-61.3
3100-10600	-41.3	-41.3
Above 10600	-51.3	-61.3

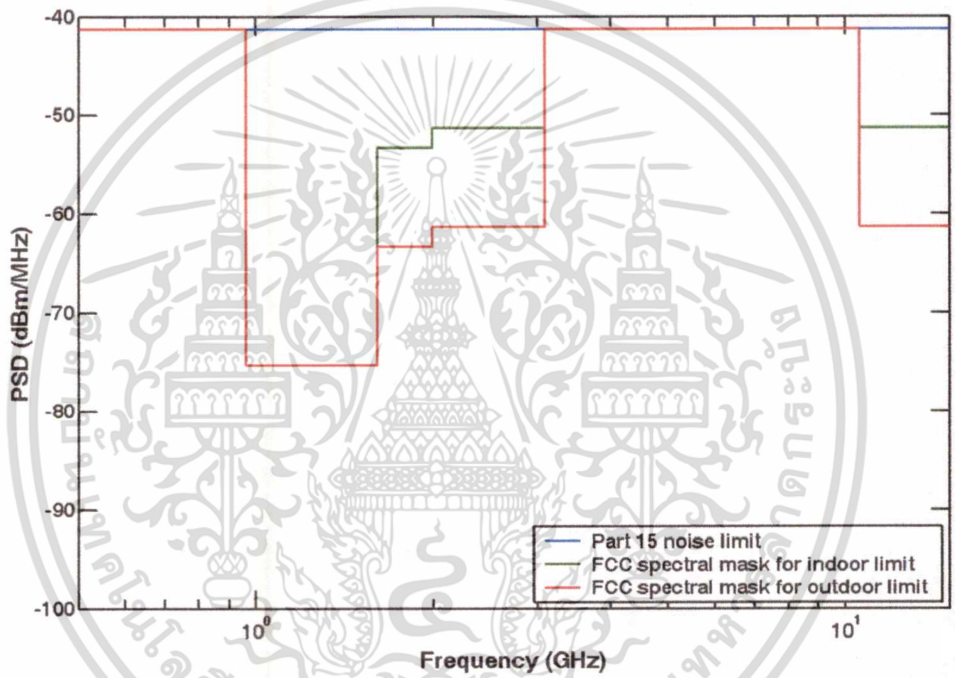

Figure 2.6 The USA spectral mark for indoor and outdoor applications [24].

2.7.2 Regulation in Europe

The European Commission (EC) has finally issued details of the licensing regulations for UWB networking in Europe. Beside the radiation limits and spectral masks specified by FCC, there are three regulations which are responsible in European regulation and standards such as: European Union (EU), European Technical Standard Institute (ETSI) and European Conference of Post and Telecommunication (CEPT). The regulation specifies PSD radiation frequency ranging from 3.1 to 10.6 GHz for indoor and outdoor communication applications as shown in table 2.3.

Table 2.3 Frist spectral masks specified by ETSI for indoor and outdoor communication applications [25].

	Frequency (GHz)		
	$f < 3.1$	$3.1 < f < 10.6$	$f > 10.6$
Indoor	$-51.3 + 87\log(f/3.1)$	-41.3	$-51.3 + 87\log(f/3.1)$
outdoor	$-61.3 + 87\log(f/3.1)$	-41.3	$-61.3 + 87\log(f/3.1)$

The new regulation of PSD radiation allows UWB-IR equipment using for an indoor application. The main frequency range is reduced to be from 6.0 to 8.5 GHz as shown in table 2.4. Figure 2.7 is the ETSI current spectral masks specified for indoor and applications.

Table 2.4 Current radiation limit specified by ETSI for indoor application [25].

Frequency (GHz)	PSD (dBm/MHz)
Less than 1.6	-90
1.6-3.8	-85
3.8-6.0	-70
6.0-8.5	-41.3
8.5-10.6	-65
Above 10.6	-85

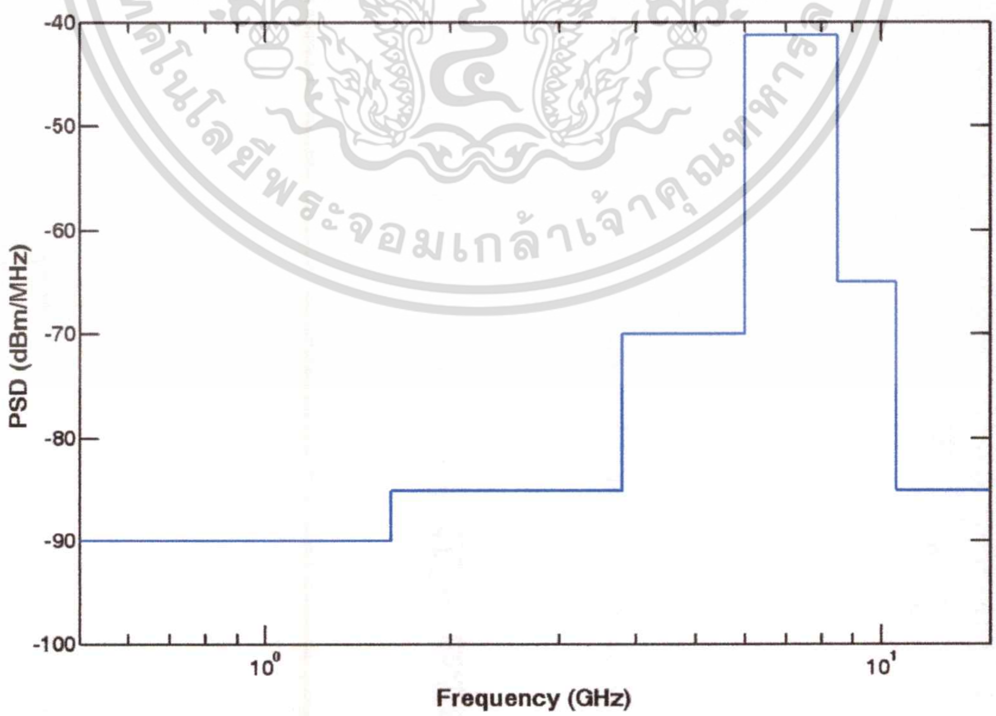

Figure 2.7 The ETSI current spectral masks specified for indoor and applications [25].

2.7.3 Common regulation

Recently, UWB-IR signal regulation has been approved in other regions as well. There is a common frequency available among FCC, ETSI and MIC. The regulation of PSD radiation is satisfied all allows FCC, ETSI and MIC regulations by using an indoor application. The main frequency range is start from 7.25 GHz to 8.5 GHz, while the lowest frequency is satisfied MIC regulation and the highest is satisfied ETSI regulation as shown in table 2.5 and the common frequency band spectral mask for indoor application is show in figure 2.8 [26].

Table 2.5 The limitation of common frequency band for indoor application [26].

Frequency (GHz)	PSD (dBm/MHz)
Less than 1.6	-90
1.6-3.8	-85
3.8-7.25	-70
7.25-8.5	-41.3
8.5-10.25	-65
10.25-10.6	-70

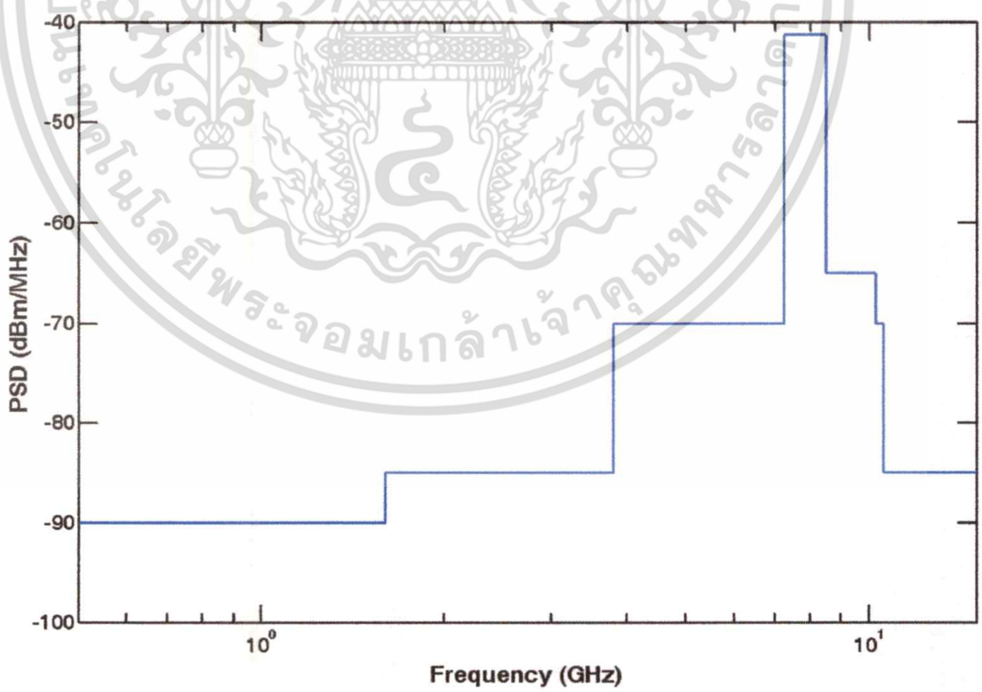

Figure 2.8 common frequency band spectral mask for indoor application [26].

2.7 Advantages of UWB

In the UWB short pulse transmission waveform, the several advantages does not use the traditional radio carriers employed by cellular, satellite, television, cable or other communications technologies. Moreover, the UWB provides the high data rates are available used in multi-user, large channel capacity due to its high band width and support real-time video streaming and low transmit power. Moreover, the UWB frequency must operate in specific slices of an increasingly crowed radio spectrum, otherwise they would interference with one another. One of the advantages of UWB is that it eliminates many of the analog components of traditional carrier wave based radios. It is an "all digital" radio. Once it is fully developed, it is destined to become a very low cost solution.

2.7 Standard and Applications of UWB

2.7.1 UWB Standard

Institute of Electrical and Electronics Engineers (IEEE) 802.15 is a working group of the IEEE 802 standards committee. There are two standards of UWB system as IEEE 802.15.3a for high rate wireless personal area networks (HR-WPANs) and IEEE 802.15.4a for low rate (LR-WPAN) [27].

IEEE 802.15.3a was formed in January 2003 with the objective of the providing a higher speed PHY layer which support data rates not exceed 480 Mbps for short distance up to 10 m [28] which involve imaging and multimedia. IEEE 802.15.3a was withdrawn in January 2006 because the members of task group were not able to decide between two technologies, multi-band orthogonal frequency division multiplexing (MB-OFDM) and direct sequence ultra-wideband (DS-UWB).

The IEEE 802.15.4 was formed in March 2004. IEEE 802.15.4a standard utilizes UWB technique for LR-WPANs for low data rate not exceed 110 Mbps and long distance up to 100 m. In this standard group use for new applications that require only moderate data throughput, but long battery life such as low-rate wireless personal area network and high accuracy localization systems. The transmitted signal is based on very short pulse and estimated to impulse, which cause the name of UWB [29].

2.7.2 UWB Application

UWB is an area that has generated a lot of interest recently and very useful for short rang communication, its multipath immunity, high data throughput, better wall penetration, low power consumption, and low probability of interception and detection. The huge and unlicensed bandwidth has been major proponent for research in this field, because of all these futures UWB has become increasingly accepted for numerous application as with innovative technologies, that can be shown in figure 2.8 as below:

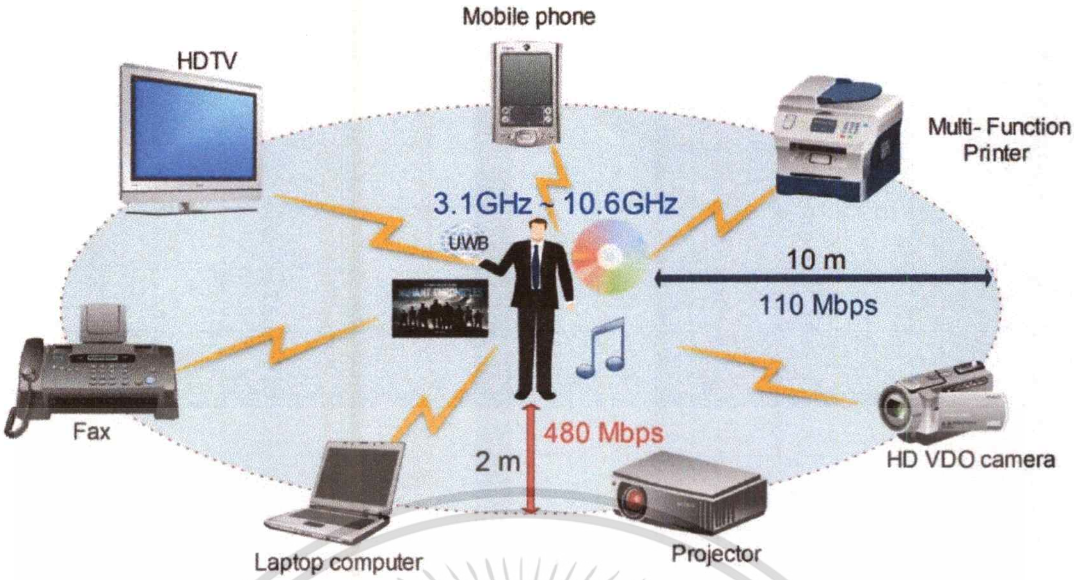

Figure 2.9 UWB for Short Rang Applications [27].

2.8 Summary.

UWB-HB communication has been presented in this chapter, we explain about history of WBAN technology, BAN regulations. It also provides a comprehensive overview of UWB-WBAN technologies and their principle components and properties. This chapter also provide a brief describe the requirements and new challenges of WBAN for medical applications. All contents are based on published standard, regulations and documents.

CHAPTER 3

THEORY AND ANALYSIS OF UWB-WBAN

3.1 Introduction

The WBAN-UWB analysis is based on the extension Friis' formula in an indoor environment. This chapter mentions theory and presented all equations use for analysis including channel transfer function (magnitude and phases), path loss, received waveform within and without matched filter, power delay profile (PDP) and bit error rate (BER) which is related to the model of experiment.

3.2 Extension Friis' Transmission Formula for UWB System

In narrowband system, the link budget of the free space propagation loss is usually estimated by using Friis' transmission formula [11] it is not directly applicable to the UWB impulse radio transmission system, as the formula expressed as a function of the frequency. Moreover, the waveform may be distorted due to the frequency characteristics of the antenna treats the special case of the constant gain and the constant aperture, but no general discussion had been made although it suggested the use of the time-domain antenna effective length.

The Friis' transmission formula has been widely used to evaluate link budget for narrow band system [11] and can be applied to the calculation of these LOS channels. The Friis' transmission gain G_{Friis} is defined as

$$G_{\mathrm{Friis}}(f) = \frac{P_{\mathrm{r}}(f)}{P_{\mathrm{t}}(f)} = G_{\mathrm{f}}(f)G_{\mathrm{r}}(f)G_{\mathrm{t}}(f) \tag{3.1}$$

$$G_{\mathrm{f}}(f) = \left(\frac{\lambda}{4\pi d}\right)^2 = \left(\frac{c}{4\pi df}\right)^2 \tag{3.2}$$

Where P_{t} is the input power of the transmitter

P_{r} is the output power of the receiver

$G_{\mathrm{t}}(f)$ is the transmitted gain

$G_f(f)$ is the free space propagation gain

$G_{\mathrm{r}}(f)$ is the received gain

$\lambda = \frac{c}{f}$ is the wavelength

c is the velocity of light

f is the operating frequency

d is the distance between transmitter and receiver antennas

It is noted that, the eq. (3.1) is satisfied at some certain frequency and it's not directly applicable to UWB systems. The Friss' transmission formula shall be extended to take into account the transmission signal waveform and it's distortion as well [31-32].

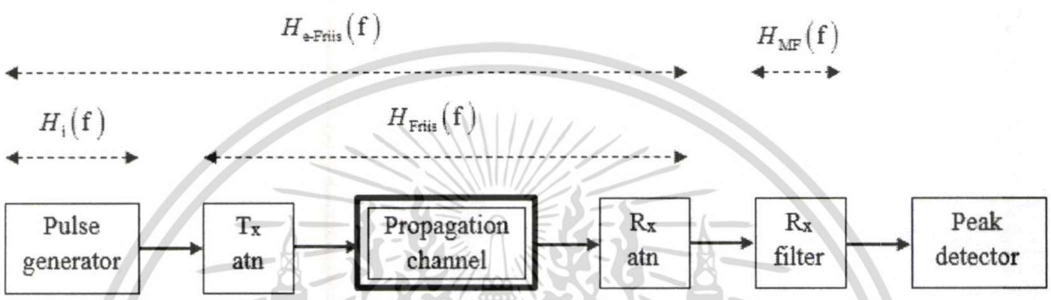

Figure 3.1 Block diagram of UWB transmission model.

The block diagram of UWB transmission model is shown in figure 3.1. The input signal $v_{\mathrm{i}}(t)$ at the transmitter port is expressed as the convolution of an impulse input the pulse shaping filter $h_{\mathrm{i}}(t)$ as

$$v_{\mathrm{i}}(t) = E_{\mathrm{i}}\delta(t) \otimes h_{\mathrm{i}}(t) \tag{3.3}$$

Where

$$\int_{-\infty}^{\infty} h_{\mathrm{i}}^{2}(t)\,\mathrm{d}t = \int_{-\infty}^{\infty} |H_{\mathrm{i}}(f)|^{2}\,\mathrm{d}f = 1 \tag{3.4}$$

Friis' formula is extended taking into account the transmission waveform for UWB system and $H_{\text{e-Friis}}(f,d)$ can be written as

$$H_{\text{e-Friis}}(f,d) = \frac{V_{\mathrm{r}}(f)}{E_{\mathrm{i}}} = H_{\mathrm{c}}(f,d)H_{\mathrm{i}}(f)\mathbf{H}_{\mathrm{r}}(f)\cdot\mathbf{H}_{\mathrm{t}}(f) \tag{3.5}$$

$$H_{\text{e-Friis},1}(f,d) = H_{\mathrm{c1}}(f,d)H_{\mathrm{i1}}(f)\mathbf{H}_{\mathrm{r1}}(f)\cdot\mathbf{H}_{\mathrm{t1}}(f) \tag{3.6}$$

$$H_{\text{e-Friis},2}(f,d) = H_{\mathrm{c2}}(f,d)H_{\mathrm{i2}}(f)\mathbf{H}_{\mathrm{r2}}(f)\cdot\mathbf{H}_{\mathrm{t2}}(f) \tag{3.7}$$

$$H_{\text{e-Friis,d}}(f,d) = H_{\text{e-Friis,1}}(f,d) + H_{\text{e-Friis,2}}(f,d) \tag{3.8}$$

Where $H_{\mathrm{f}}(f,d)$ is free space transfer function

$\mathbf{H}_{\mathrm{r}}(f)$ is complex transfer function vector of received antenna

$H_{\mathrm{i}}(f)$ is pulse generation function

$\mathbf{H}_{\mathrm{t}}(f)$ is complex transfer function of transmitted antenna

$E_{\mathrm{i}} = 1$ is the output waveform

$$\mathbf{H}_{\mathrm{a}}(f) = \mathbf{H}_{\mathrm{a}}(\theta_{\mathrm{a}},\varphi_{\mathrm{a}},f) = \hat{\theta}\mathbf{H}_{\mathrm{a}\theta}(\theta_{\mathrm{a}},\varphi_{\mathrm{a}},f) + \hat{\varphi}\mathbf{H}_{\mathrm{a}\theta}(\theta_{\mathrm{a}},\varphi_{\mathrm{a}},f) \tag{3.9}$$

Where $\mathbf{H}_{\mathrm{a}}$ (a = r or t) is a complex transfer function vector of antenna relative to the isotropic antenna

The eq. (3.9) is a complex transfer function vector of the antenna relative to the isotropic antenna. The free space transfer function $H_{\mathrm{f}}(f,d)$ can be written as

$$H_{\mathrm{f}}(f,d) = \frac{\lambda}{4\pi d}\exp(-jkd) \tag{3.10}$$

Eq 3.10 is the free space transfer function where

$$k = \frac{2\pi}{\lambda} \tag{3.11}$$

Eq. 3.11 is the propagation constant. The received waveform $v_{\mathrm{r}}(t,d)$ can be considered by using

$$v_{\mathrm{r}}(t,d) = v(t) \otimes h_{\mathrm{Friis}}(t,d) \tag{3.12}$$

Where $v(t)$ is the transmitted signal waveform,

$\otimes$ is the convolution operator

$h_{\mathrm{Friis}}(t,d)$ is the impulse response of the extension of Friis' formula

3.3 UWB Received Waveform

The spectral density of UWB received signal V_{r} is calculated by using multiplication between H_{f} and V_{t}, which can be written as

$$V_{\mathrm{r}}(f)=V_{\mathrm{t}}(f)H_{\mathrm{f}}(f) \tag{3.13}$$

UWB received waveform in time domain, we can obtained the received by using invert Fourier transform (IFT) of spectral density which can be written as

$$v_{\mathrm{r}}(t)=\int_{-\infty}^{\infty} V_{\mathrm{r}}(f)e^{j2\pi ft}df \tag{3.14}$$

3.4 Matched Filter Receiver

At the receiver, the matched filter is introduced to maximize the SNR of the receiver output. The matched filter with frequency transfer functions satisfied constant noise power condition between input and output are considered. The block diagram of the matched filter system is shown in figure 3.2 as below:

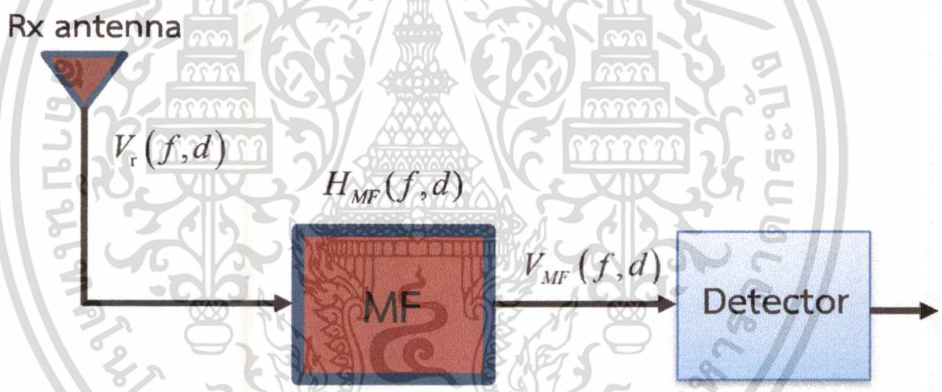

Figure 3.2 Block diagram of matched filter receiver.

The spectral density of the signal waveform at the output of the matched filter $V_{MF}(f,d)$ can be calculate by using the transfer function of matched filter $H_{MF}(f,d)$ multiply by the spectral density function of the received waveform $V_{\mathrm{r}}(f,d)$ as

$$V_{MF}(f,d)=H_{MF}(f,d)\cdot V_{\mathrm{r}}(f,d) \tag{3.15}$$

The frequency transfer functions of matched filter can be written as

$$H_{\mathrm{MF}}(f)=\frac{H^{*}_{\mathrm{e-Friis}}(f)}{\sqrt{\int_{-\infty}^{\infty}\left|H^{*}_{\mathrm{e-Friis}}(f)\right|^{2}\mathrm{d}f}} \tag{3.16}$$

And the Matched Filter in case of Isotropic can be defined as

$$H_{\text{MF,Iso}}(f) = \frac{H^{*}_{\text{e-Friis}}(f)}{\sqrt{\int_{-\infty}^{\infty} \left|H^{*}_{\text{e-Friis}}(f)\right|^{2} df}} \tag{3.17}$$

Where $(\cdot^{*})$ is the complex conjugate

Which satisfies the following constant noise output power condition from the eq (3.16) H_{MF} is normalized as

$$\int_{-\infty}^{\infty} \left|H_{\text{MF}}(f)\right|^{2} \mathrm{d}f = 1 \tag{3.18}$$

In this case, the spectrum of the receiver output are $h_{\text{e-Friis}}(t)$ and $H_{\text{e-Friis}}(f)$ respectively. After we obtained the spectral density function at the output signal of the matched filter receiver waveform $v_{\text{MF}}(t)$ by using inverse Fourier transform, can be written as

$$\begin{aligned} v_{\text{MF}}(t) &= h_{\text{e-Friis}}(t) \otimes h_{\text{MF}}(t) \\ &= \frac{\sqrt{2 f_{\text{b}}}\, h_{\text{e-Friis}}(t) \otimes h_{\text{e-Friis}}(-t)}{\sqrt{\int_{-\infty}^{\infty} h^{2}_{\text{e-Friis}}(t) dt}} \end{aligned} \tag{3.19}$$

For the in case of Isotropic can be written as

$$\begin{aligned} v_{\text{MF,Iso}}(t) &= h_{\text{e-Friis,Iso}}(t) \otimes h_{\text{MF,Iso}}(t) \\ &= \frac{\sqrt{2 f_{\text{b}}}\, h_{\text{e-Friis,Iso}}(t) \otimes h_{\text{e-Friis,Iso}}(-t)}{\sqrt{\int_{-\infty}^{\infty} h^{2}_{\text{e-Friis,Iso}}(t) dt}} \end{aligned} \tag{3.20}$$

For the output spectral density from matched filter $V_{\text{MF}}(f)$. It obtained as

$$\begin{aligned} V_{\text{MF}}(f) &= H_{\text{e-Friis}}(f) H_{\text{MF}}(f) \\ &= \frac{\sqrt{2 f_{\text{b}}} \left|H_{\text{e-Friis}}(f)\right|^{2}}{\sqrt{\int_{-\infty}^{\infty} \left|H_{\text{e-Friis}}(f)\right|^{2} df}} \end{aligned} \tag{3.21}$$

Taking its maximum as

$$\max_{t} v_{\mathrm{MF}}(t) = v_{\mathrm{MF}}(0) = \int_{-\infty}^{\infty} V_{\mathrm{MF}}(f)df \\ = \sqrt{2f_{\mathrm{b}} \int_{-\infty}^{\infty} \left|H_{\mathrm{e-Friis}}(f)\right|^2 df} \tag{3.22}$$

Eq. (3.22) is the UWB extension of Friis' transmission formula [11]. It includes three elements, namely the frequency characteristics of the antennas, the frequency characteristics of free space propagation, and the spectrum of the transmit signal. It is clear from eq. (3.22) that the transmission gain of the UWB signal cannot be defined as the product of gains of antennas and a free space channel as Friis' formula (3.22). Instead, the total transmission gain including the effect of the waveform can be obtained as eq. (3.22). For the normalization, the reference isotropic antenna with $H_{\mathrm{Iso}}(f) = 1$ is considered.

3.5 Path Loss

In the wireless communication system the important parameter use for analyzing the channel propagation that is path loss. Path loss model represents the attenuation of the signal as a function of the distance between the Tx and Rx antennas. Due to propagation channel by consider the propagation of UWB signal in indoor environments is an important issue with significant impacts on the future direction and scope of the UWB technology and its applications. The distance dependent path loss PL can be expressed by eq. (3.23) as

$$PL[dB] = 20\log\left[\frac{v_{\mathrm{t}}(t)}{v_{\mathrm{r}}(t)}\right] \tag{3.23}$$

Where $v_{\mathrm{t}}(t)$ is the transmitted signal waveform

$v_{\mathrm{r}}(t)$ is the received signal waveform

For the UWB path loss we consider at transmitted signal maximum power and received signal maximum power as function of distance d

$$PL_{\mathrm{UWB}}(d)[dB] = 20\log\left[\frac{\max|v_{\mathrm{t}}(t)|}{\max|v_{\mathrm{r}}(t,d)|}\right] \tag{3.24}$$

From eq. (3.24) we define the transmitted signal equal 1. Therefore, we can rewrite equation as following

$$PL_{\mathrm{UWB}}(d)[dB] = -20\log[\max|v_{\mathrm{r}}(t,d)|] \tag{3.25}$$

3.6 Power Delay Profile (PDP)

Power delay profile (PDP) represents the power received signal as a function of time. The channel impulse responses are obtained by IFFT (Inverse Fast Fourier Transform) of recorded transfer functions. A Hamming window is applied in frequency domain to reduce the side lobes in the time domain. Mean excess delay $\bar{\tau}$ is the averaged delay weighted by power and is calculated as (3.26)

$$\bar{\tau} = \frac{\sum_{\mathrm{i=1}}^{\mathrm{n}} a_{\mathrm{i}}^2 \tau_{\mathrm{i}}}{\sum_{\mathrm{i=1}}^{\mathrm{n}} a_{\mathrm{i}}^2} = \frac{\sum_{\mathrm{i=1}}^{\mathrm{n}} P(\tau_{\mathrm{i}})\tau_{\mathrm{i}}}{\sum_{\mathrm{i=1}}^{\mathrm{n}} P(\tau_{\mathrm{i}})} \tag{3.26}$$

Root Mean Square delay τ_{RMS} is the energy-weighted standard deviation of signal delay can be written as

$$\tau_{\mathrm{RMS}} = \sqrt{\overline{\tau^2} - (\bar{\tau})^2} \tag{3.27}$$

$$\overline{\tau^2} = \frac{\sum_{\mathrm{i=1}}^{\mathrm{n}} a_{\mathrm{i}}^2 \tau_{\mathrm{i}}^2}{\sum_{\mathrm{i=1}}^{\mathrm{n}} a_{\mathrm{i}}^2} = \frac{\sum_{\mathrm{i=1}}^{\mathrm{n}} P(\tau_{\mathrm{i}})\tau_{\mathrm{i}}^2}{\sum_{\mathrm{i=1}}^{\mathrm{n}} P(\tau_{\mathrm{i}})} \tag{3.28}$$

Where a_{i} is the signal level of path i

τ_{i} is time delay of path i

$P(\tau_{\mathrm{i}})$ is the signal power of path i

3.7 Bit Error Rate (BER)

The BER is defined as the rate at which error occur in a transmission can consider from correlation coefficient between received signals with template waveform [33].

The correlation coefficient of correlation coefficient of template waveform C_c can show as

$$C_c = \frac{\max|r_{ab}(\tau)|}{\sqrt{\max|r_a(\tau)| \bullet \max|r_b(\tau)|}} \tag{3.29}$$

The BER can be expressed as equation 3.30

$$BER = Q\left(\sqrt{2C_c\left(E_b/N_o\right)}\right) \tag{3.30}$$

Where $r_a(\tau)$ is the auto-correlation of signal a

$r_b(\tau)$ is the auto-correlation of signal b

$r_{ab}(\tau)$ is the cross correlation function between signal a and b

E_b/N_o is the energy per bit to noise power spectral density ratio

Q is the Q – function which is obtained from eq. (3.31)

$$Q(x) = \frac{1}{x\sqrt{2\pi}} e^{-x^2} / 2 \; ; \; x \geq 0 \tag{3.31}$$

3.8 Summary

This chapter discusses theory and some parameters used for UWB channel propagation for wireless communication system, based on the extension Friis' formula in an indoor environment. This chapter presented all equations use for analysis are including path loss, received waveform, power delay profile, bit error rate and other parameters, were used to analyses an effects from power loss and distortion of signal. These effect are caused by multipath and absorption which are in between the transmitter and receiver.

CHAPTER 4
EXPERIMENTAL EVALUATION OF UWB-HB TRANSMISSION WAVEFORM

4.1 Introduction

In this chapter, describes the experimental setup and channel measurement model for UWB-WBAN propagation were used in the experiment. The main equipment is vector network analyzer (VNA), the meander line antennas are used as a transmitter (Tx) and receiver (Rx) antennas, a characteristic of meander line antenna, parameters, UWB transmission waveform and also dimension the experiment an indoor environment.

4.2 Measurement Setup

The experiment conducted in this work is based on a model of a BAN holding six node on-body sensors by using VNA, which has defined two different sets of measurements as single and double transmission waveform. Both of transmitter and receiver are meander line antenna and fix the frequency range from 3 GHz to 10.6 GHz. The measurement setup in this thesis is shown in figure 4.1. For all important parameters are also describes of each section.

4.3 Equipment of Experiment

The main equipment of this experiment not only including hardware but also software as list below:

- Hardware
    1) Vector Network Analyzer (VNA)
    2) Meander Line Antenna
    3) Calibration Kits
    4) Cable line
    5) Computer
    6) Others devices
- Software
    1) Matlab Program

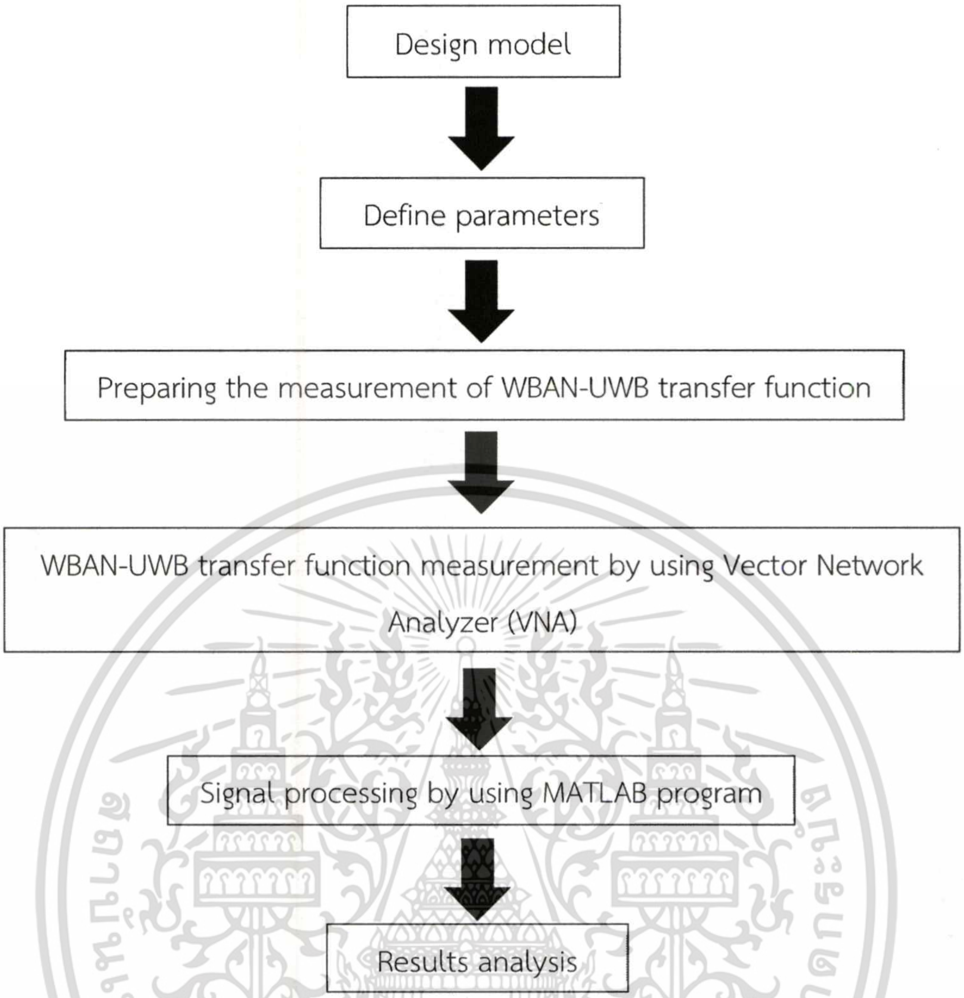

Figure 4.1 Block diagram of measurement evaluation.

4.3.1 Vector Network Analyzer (VNA HP-8510C)

VNA is utilized to measure S-parameter which corresponds to a channel transfer function, where Port1 is transmitter (Tx) port and port 2 is receiver (Rx) port. Respectively, VNA consist of the vector network circuit analyzer model HP-8510C [34], S-parameter test set model HP-8514B, an HP-8510C network analyzer as an intermediate frequency (IF) receiver, meander line antennas as transmitting and receiving antennas, IBM PC-compatiible computer with MATLAB as a data acquisition workstation and frequency synthesized sweeper model HP-83620A is main instrument show as figure 4.2.

VNA devices are operating in single-sweep stepping mode, sweeping the predefined frequency band using 801 points. The weeping time is automatically adjusted by the analyzer, depending on the bandwidth and on the number of measured frequency point within the sweeping band. Moreover, the VNA require a calibration with the same cables and adapters as will be used in the measurement.

For each frequency step, the system is continuous-wave signals are transmitted though the transmitting antenna in an indoor environment. The RF energy reflected by the target is collected by the receiving antenna.

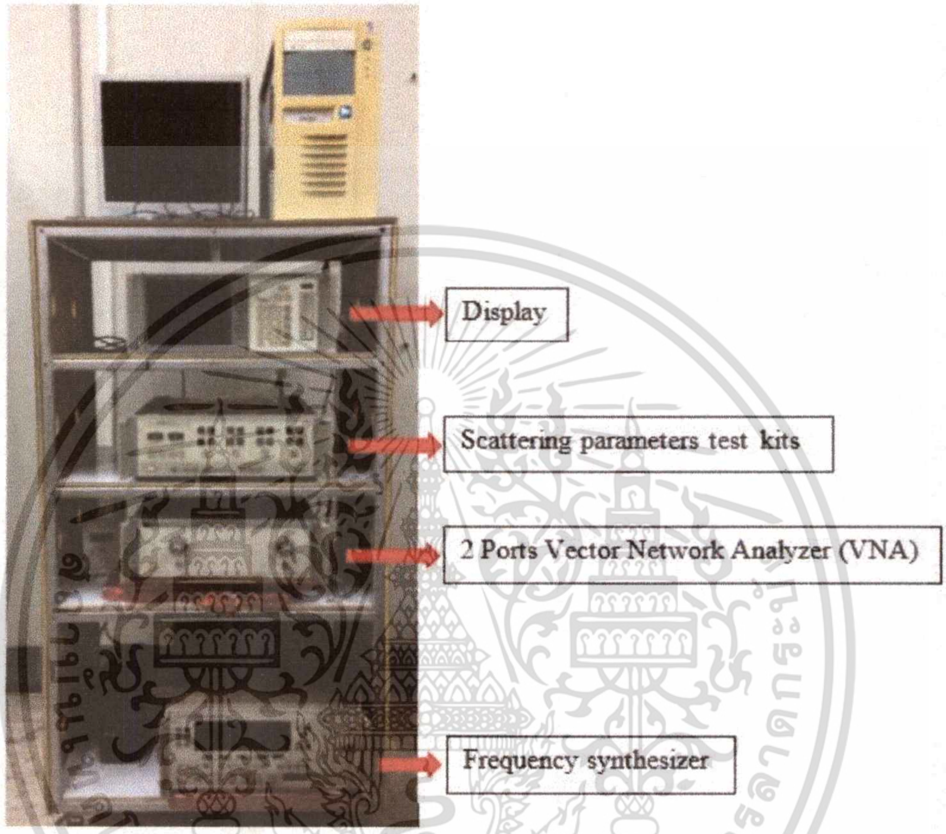

Figure 4.2 Vector Network Analyzer.

4.3.2 Meander Line Antenna

In wireless communication, antenna is very important equipment for transmitting and receiving signals. The design criteria for WBAN antenna should be small physical size. Hence, The Meander line antenna is a small antenna as 16x13.6x3 mm and transducer designed to transmit or receive electromagnetic waves in UWB frequency by Sky-Cross Company, United State. And it's a one of the commercial product [35]. The geometric and dimension of the meander line is shown in figure 4.3 and absolute |S11| of Meander line Antenna is shown in figure 4.4. For the radiation pattern of the meander line is omni-directional and the frequency range from 3.1 GHz-10.6 GHz for UWB approved by the FCC in 2002. The meander line antenna and characteristic of the refection coefficient S_{11} of the antenna in UWB frequency is below -10 dB.

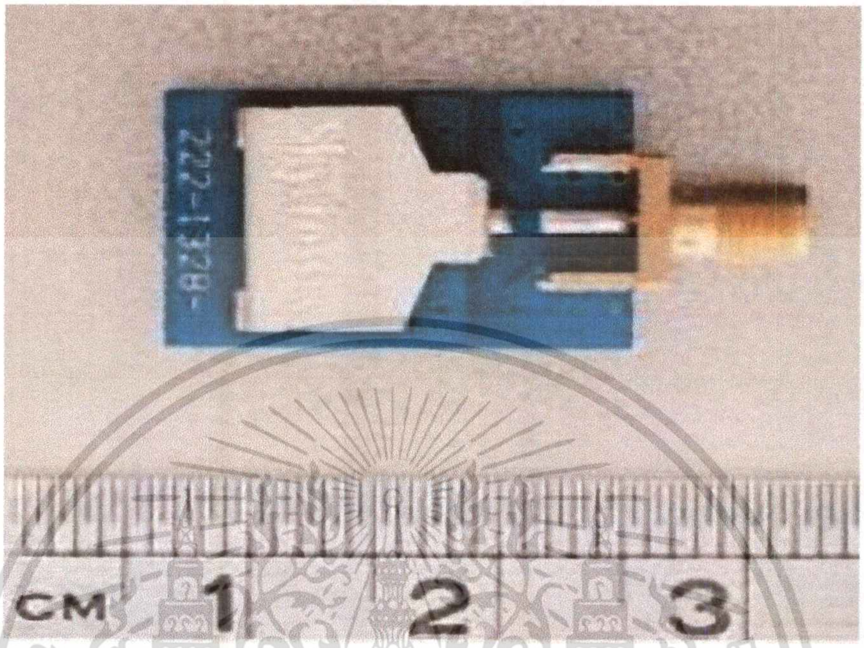

Figure 4.3 Meander line Antenna [35].

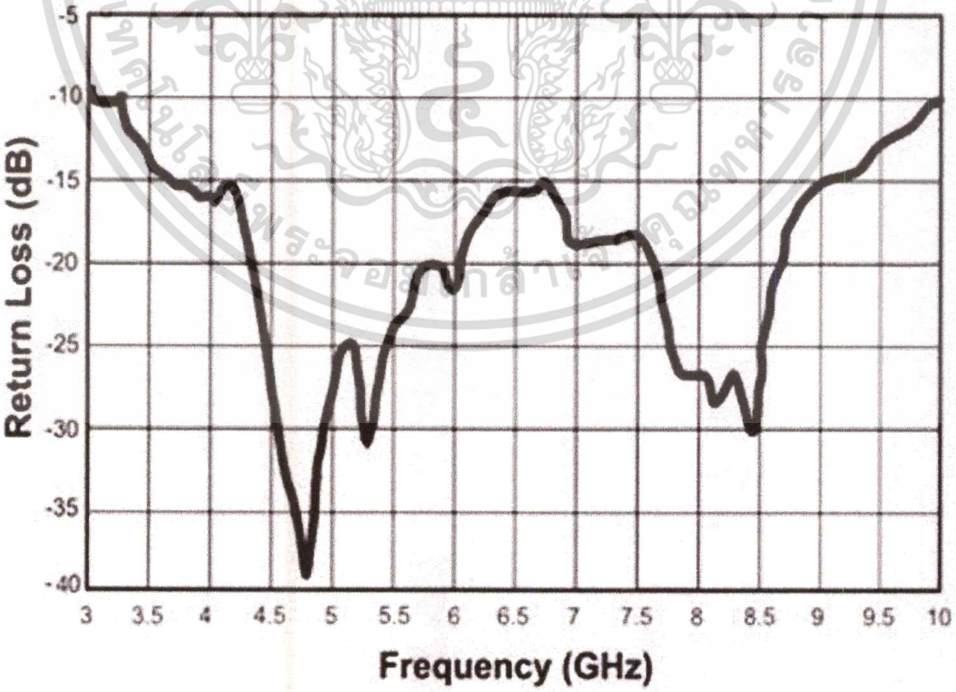

Figure 4.4 Absolute $|s_{11}|$ of Meander line Antenna [35].

4.3.3 Rectangular Waveform

For UWB transmission signal waveform, the rectangular passband waveform [36] is considered as the UWB transmission signal. The expression of UWB transmission signal (V_t) in time domain frequency domain are given by eq. (4.1) and eq. (4.2). respectively. The transmitted signal waveform and spectrum of UWB are shown in figure 4.5. And figure 4.6.

$$v_{\mathrm{t}} = \frac{1}{f_{\mathrm{b}}}[f_{\mathrm{H}} \sin c(2f_{\mathrm{H}}t) - f_{\mathrm{L}} \sin c(2f_{\mathrm{L}}t)] \tag{4.1}$$

$$V_{\mathrm{t}}(f) = \begin{cases} \dfrac{A}{2f_{\mathrm{b}}} \left\| f \right| - f_{\mathrm{c}} \right| \le \dfrac{f_{\mathrm{b}}}{2} \\ 0 \left\| f \right| - f_{\mathrm{c}} \right| > \dfrac{f_{\mathrm{b}}}{2} \end{cases} \tag{4.2}$$

Where t is the time

A is maximum amplitude

f is frequency

f_{H} is maximum frequency [10.6 GHz]

f_{L} is minimum frequency [3.1 GHz]

f_{b} is occupied bandwidth [7.5 GHz]

f_{c} is center frequency

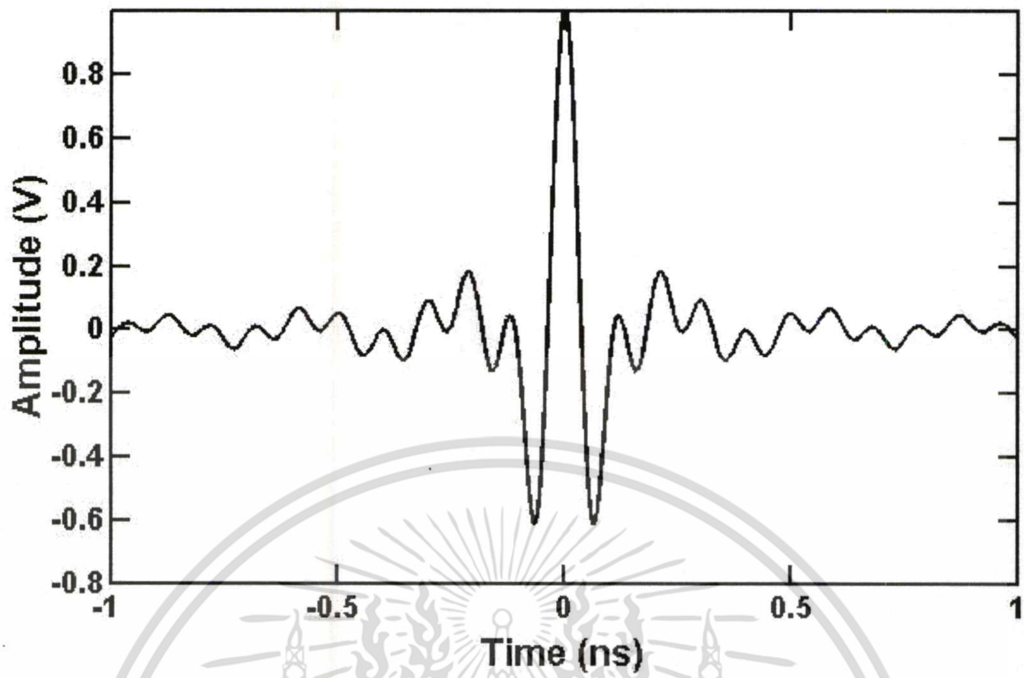

Figure 4.5 Rectangular passband waveform in time domain.

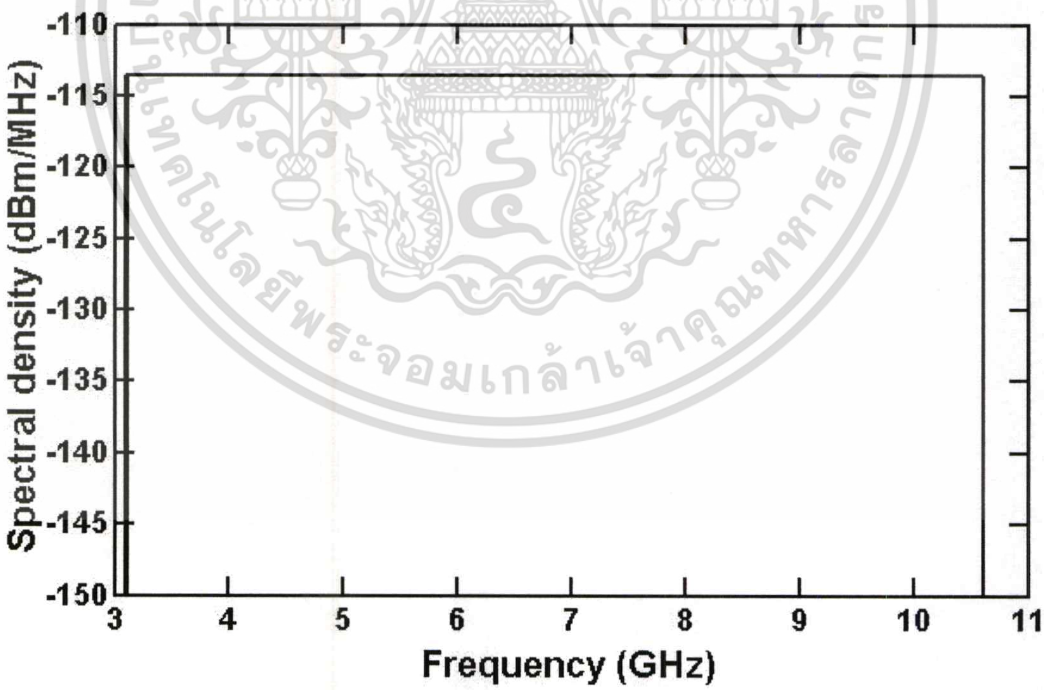

Figure 4.6 Rectangular passband waveform in frequency domain.

4.4 Simulation Parameters

The important parameters of measurements are listed in table 4.1. It is note that the calibration of VNA was done at the connectors of the cables to be connected to the antennas, in the frequency range from 3 GHz to 10.3 GHz and the number of measure frequency point per sweep 801. Therefore, all impairments of the antenna characteristics are included in the measurement results.

Table 4.1 All important parameters of experiments.

Parameter	Value
Frequency range	3 GHz to 10.6 GHz
Number of point	801 points
Antenna type	Meander line
Antenna polarization	Horizontal
Intermediate frequency (IF)	2.5 MHz
Tx antenna height	1 m

4.5 Measurement Model

In this part, the measurements were described the details of measurements setup, It can be possible to send 2 data at the same time by connecting Tx antennas to Rx antenna. The double transmitter and a single receiver were set in horizontal plane and used as middle line antennas. The transfer function were measured by using VNA.

Table 4.2 Antenna height and the distance of Tx and Rx antennas on human body.

position	Tx antenna height	Distance of Tx and Rx antennas
1	1.3 m	0.3 m
2	1.38 m	0.38 m
3	1.2 m	0.23 m
4	0.8 m	0.2 m
5	0.4 m	0.6 m

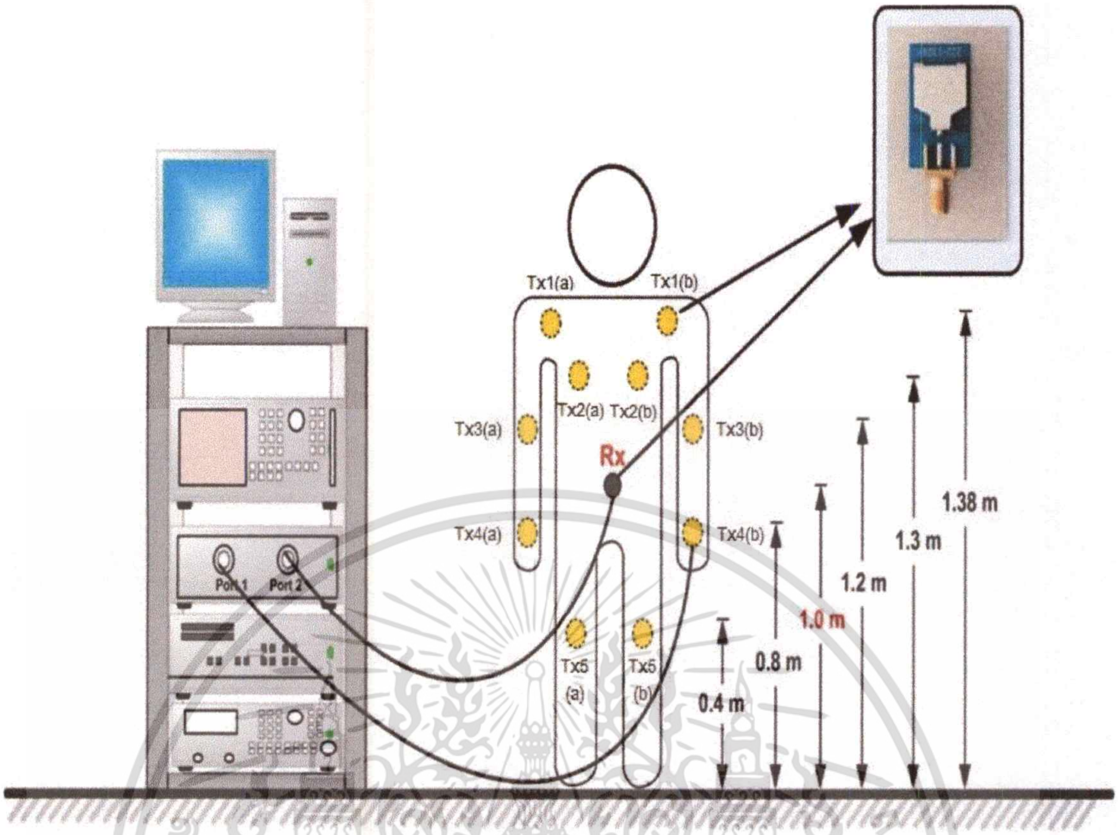

Figure 4.7 Measurement Model.

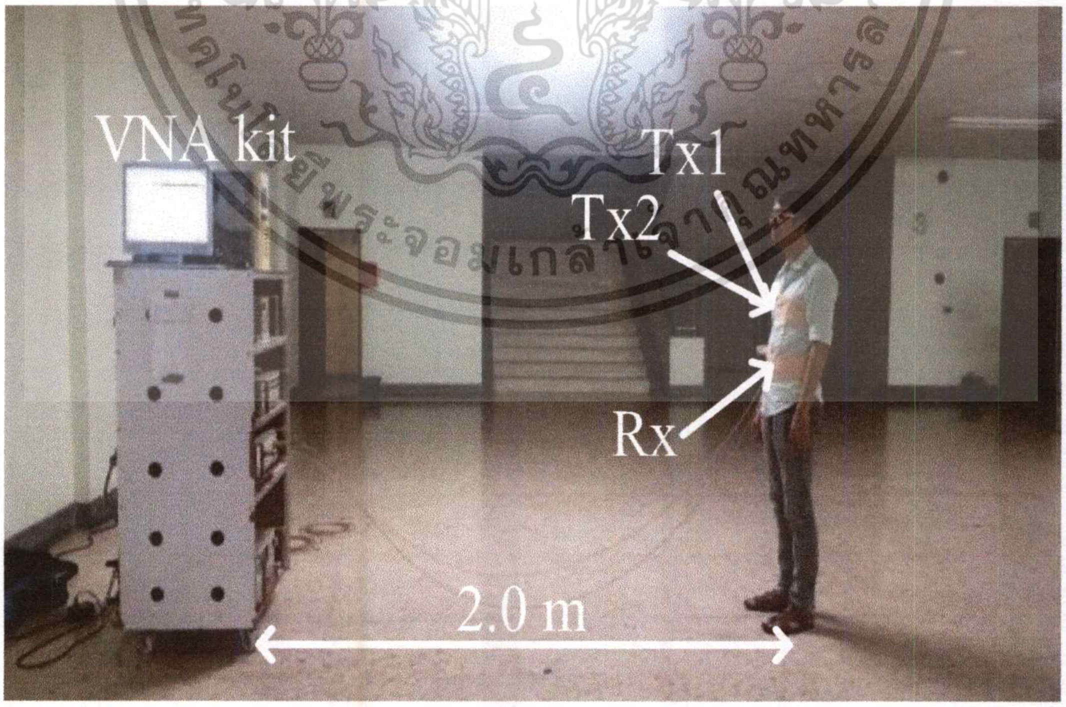

Figure 4.8 measurement site setup.

The measurement were carried out using a four-port VAN, which applied to measure magnitude and phase of the transmission confident. The VNA was operated in the response measurement mode where port1 and port 2 were transmitter receiver ports, respectively. The full 2-port method was utilized to calibrate the analyzer to suppress the noise level and improve the sensitivity and accuracy measurement. In the measurement, both of Tx and Rx antenna are meander line antennas (SMT-3TO10M-A) by Skycross company, which are commercial antennas involved and design for on-body communication. During the measurement campaign, the antenna were attached to a human body, the double transmitter antennas ($Tx_{(a)}$,$Tx_{(b)}$) were placed at left and right sides of chest, shoulder, elbow, wrist, knee of each pair on human body positions, respectively. A receiver antenna was attached to the navel on a human body, like measurement model in figure 4.7. The distance between Tx and Rx antennas height are shown in table 4.2. In addition, this work was experimented in an indoor environment at the empty room of 12 KMITL building without other wireless sources and anybody in order to ensure the statistically stationary of channel propagation as shown in figure 4.8.

4.6 Summary

The main purpose of this chapter is to make the concept of UWB-WBAN. Which is introduced the experiment and equipment in this thesis. The measurement setup was done by using VNA, UWB meander line antennas and others equipments. Finally, the results discussion will be explain in chapter 5.

CHAPTER 5
RESULTS AND DISCUSSION

5.1 Introduction

The measurement results for the parametric channel modelling by using meander line antenna at the transmitter and receiver are given in this chapter. The results of experimental based on measurements data consist of the antennas were placed at difference positions on the body to compared single and double transmission waveform results. As the results will be shown channel transfer function (magnitude and phase), path loss, received waveform in case of within and without matched filter, power delay profile and bit error rate are compared of single and double transmission waveform.

5.2 Magnitude and Phase of Channel Transfer Function

5.2.1 Magnitude

This section describes the related results of channel transfer function and phase, as a magnitude response of chest, shoulder, elbow, wrist and knee positions, respectively. The measured $|S_{21}|$ is actually the multiplication of transfer functions of Tx and Rx antennas which are separated by 30 cm, 38 cm, 23 cm, 20 cm and 60 cm from navel (Tx) to 5 positions on body (Rx, as mentioned above), respectively. Hence, we can observe the double transmitting antenna is higher than the single transmitting antenna as shown in figures 5.1 to 5.5, respectively. Therefore, the investigated and provided double transmitting signal waveform can be improved a side effect caused by the body. From results, the magnitudes of channel transfer function between single and double directional transmission on chest position are difference based on frequency characteristics.

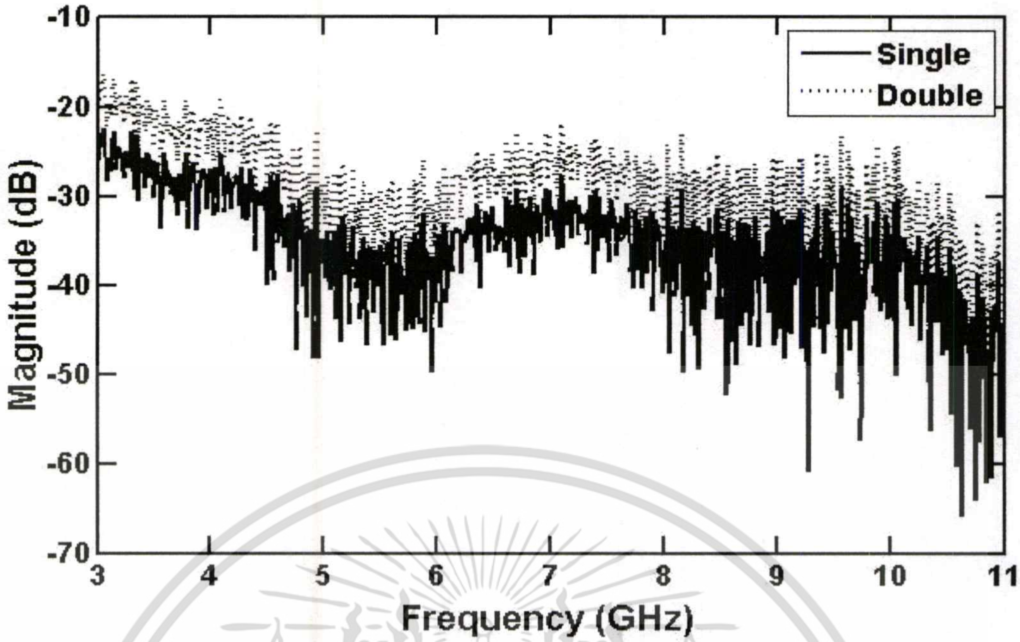

Figure 5.1 The comparison of channel transfer function between single and double directional transmission on chest position; magnitude.

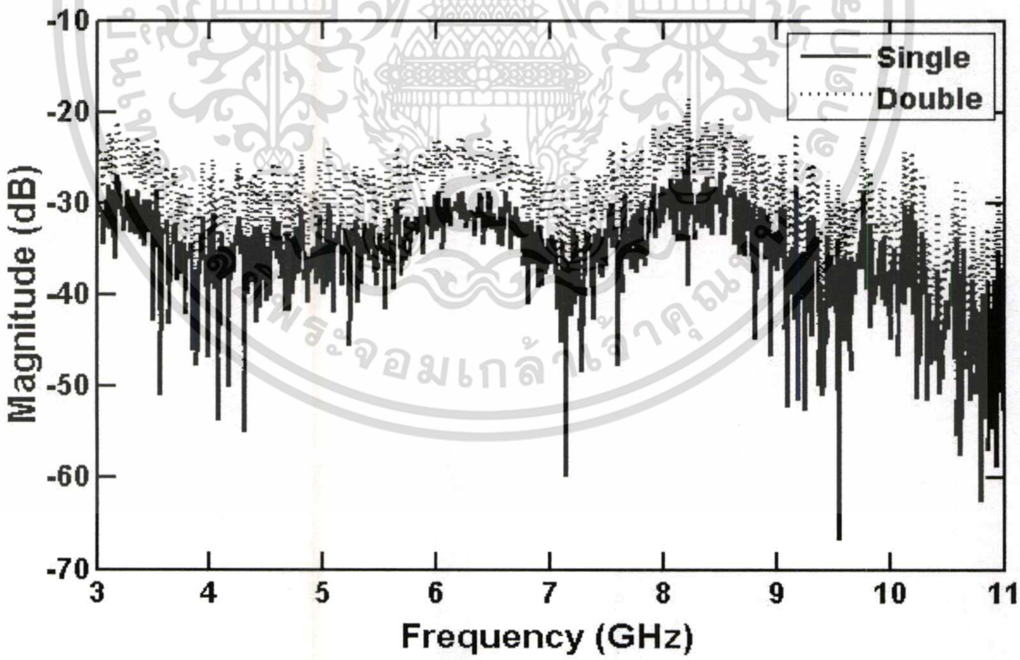

Figure 5.2 The comparison of channel transfer function between single and double directional transmission on shoulder position; magnitude.

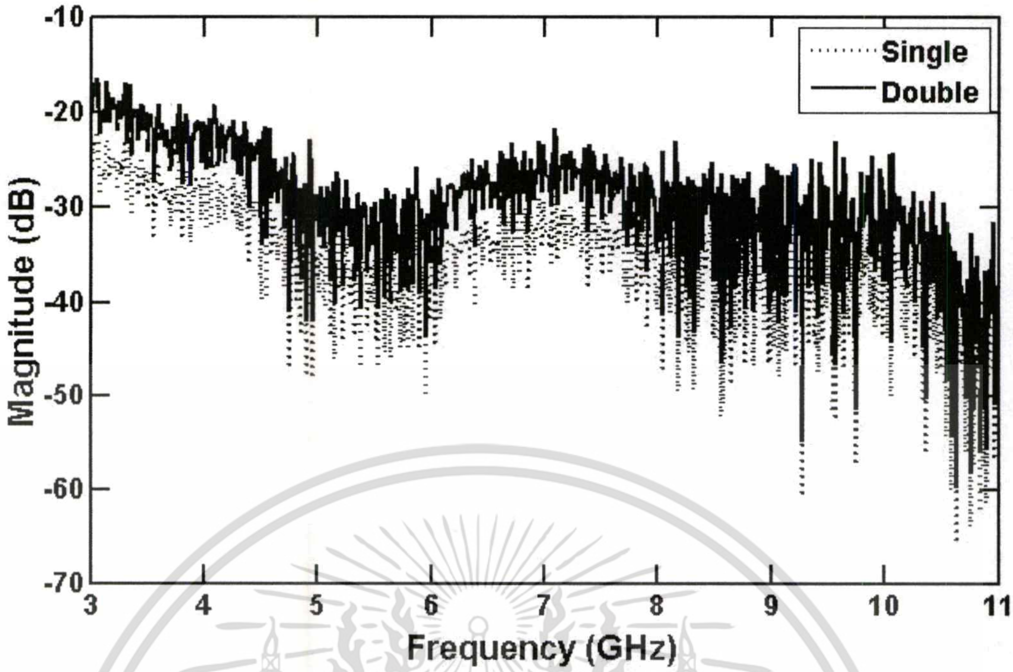

Figure 5.3 The Comparison of channel transfer function between single and double directional transmission on elbow position; magnitude.

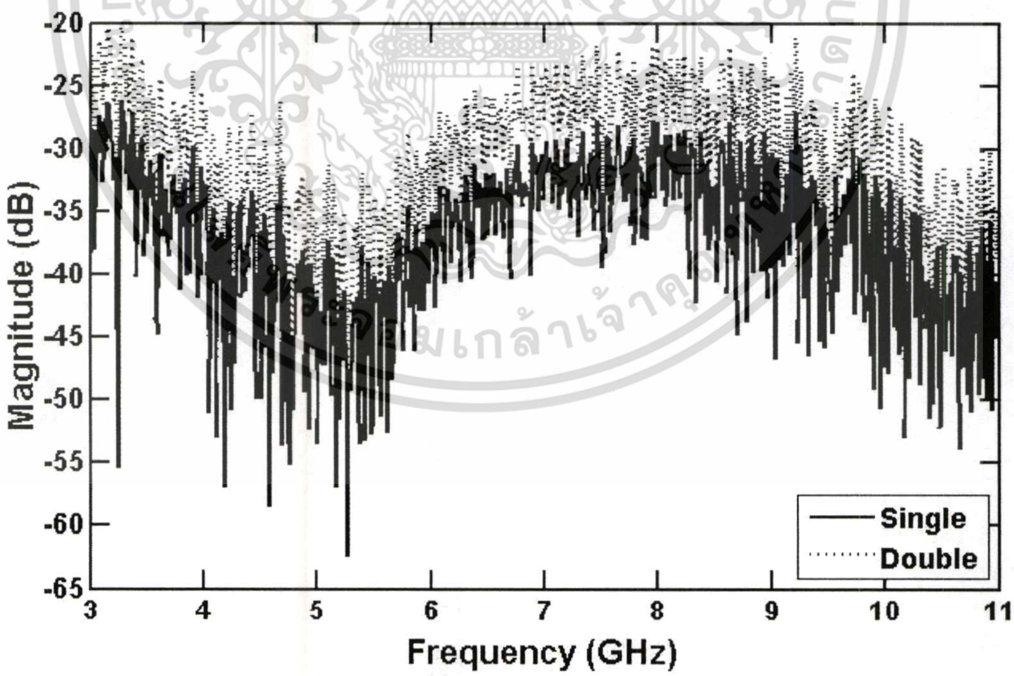

Figure 5.4 The Comparison of channel transfer function between single and double directional transmission on wrist position; magnitude.

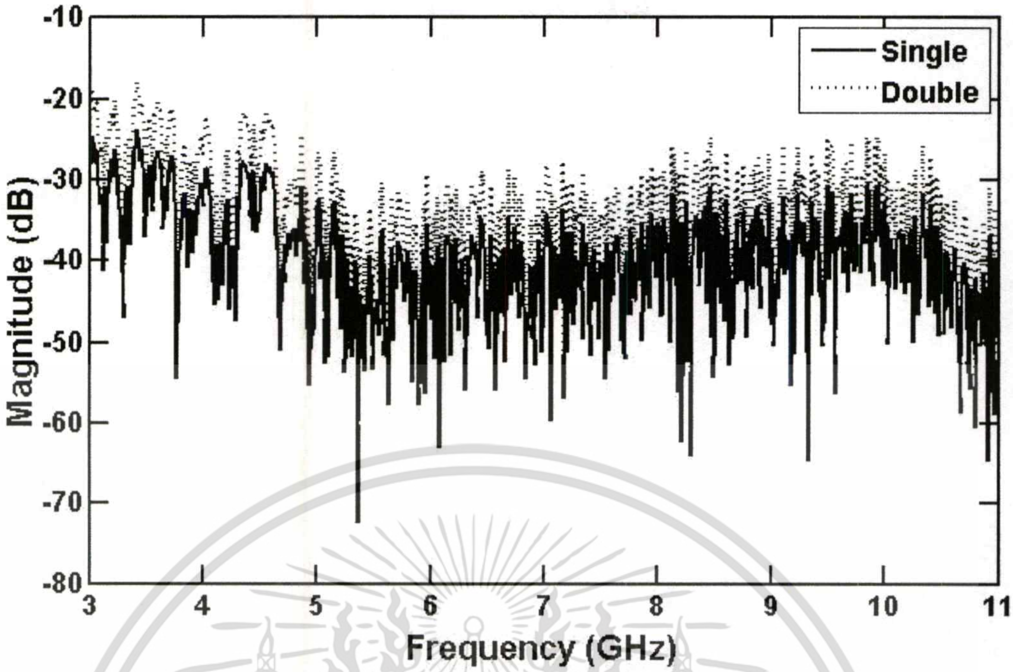

Figure 5.5 The comparison of channel transfer function between single and double directional transmission on knee position; magnitude.

Table 5.1 Comparison of single and double channel transfer function; magnitudes

Position	Magnitude Max (dB)		Magnitude Min (dB)		Magnitude Mean (dB)	
	Single	Double	Single	Double	Single	Double
1	-47.89	-23.86	-63.88	-57.86	-55.88	-40.86
2	-25.82	-18.41	-66.6	-60.58	-46.21	-39.49
3	-22.25	-16.32	-65.73	-59.71	-43.99	-38.01
4	-26.59	-20.23	-62.33	-56.31	-44.46	-38.27
5	-24.7	-17.79	-72.34	-66.32	-48.53	-42.05

From table 5.1 the comparison of single and double directional transmission channel transfer function in magnitudes to know that double directional transmission better than single directional transmission at all positions.

5.2.2 Phase

In this section, the comparison of single and double transmitting antennas are performed based on the results presented from figure 5.10 to 5.14 shows phase results between single and double directional transmission waveform of frequency transfer function of channel at position number 1 to 5, respectively. Results shows that almost phase results are linear from 3 GHz to 9 GHz, caused from the characteristics of the antenna accepted the corresponding frequency.

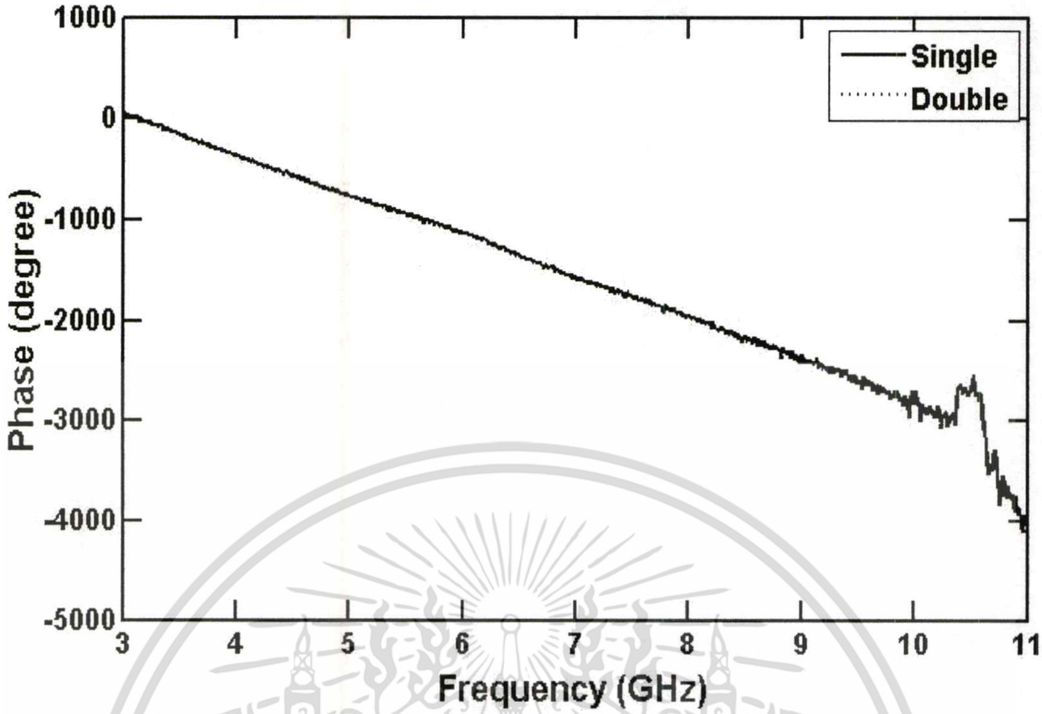

Figure 5.6 The comparisons of channel transfer function between single and double directional transmission on chest position; phase.

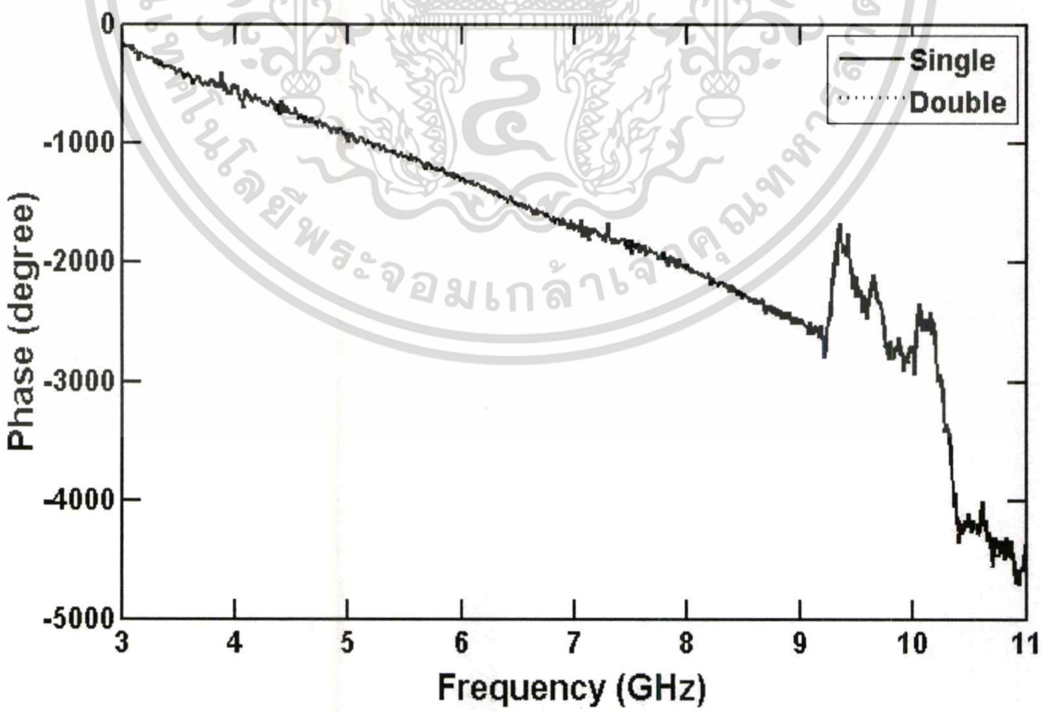

Figure 5.7 The comparisons of channel transfer function between single and double directional transmission on shoulder position; phase.

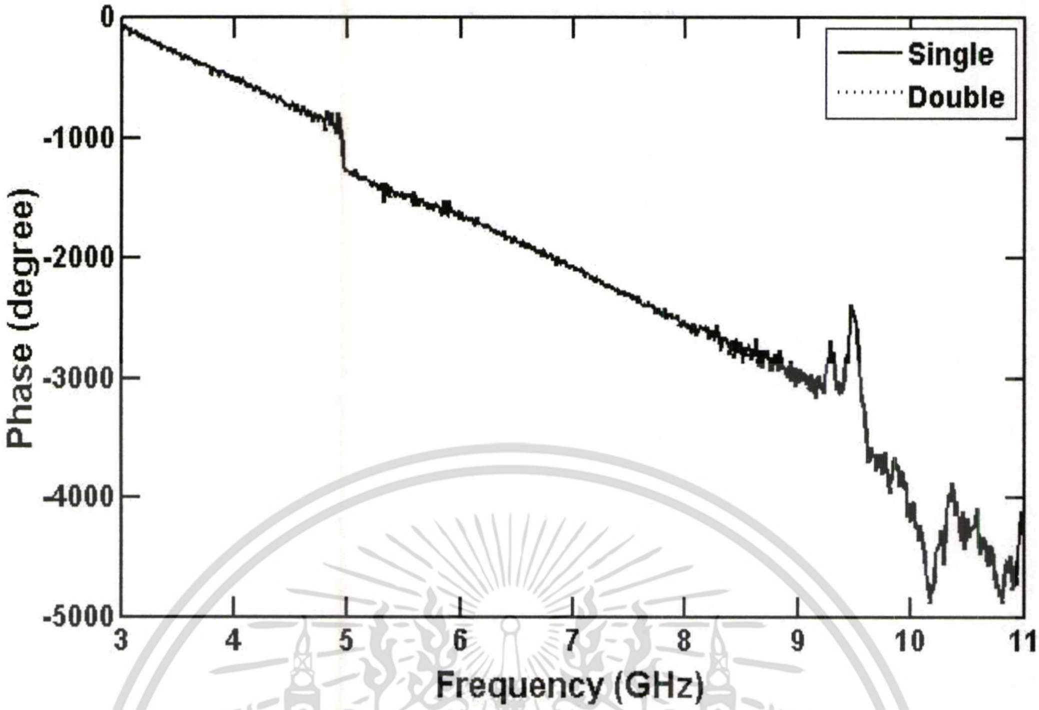

Figure 5.8 The comparisons of channel transfer function between single and double directional transmission in elbow position; phase.

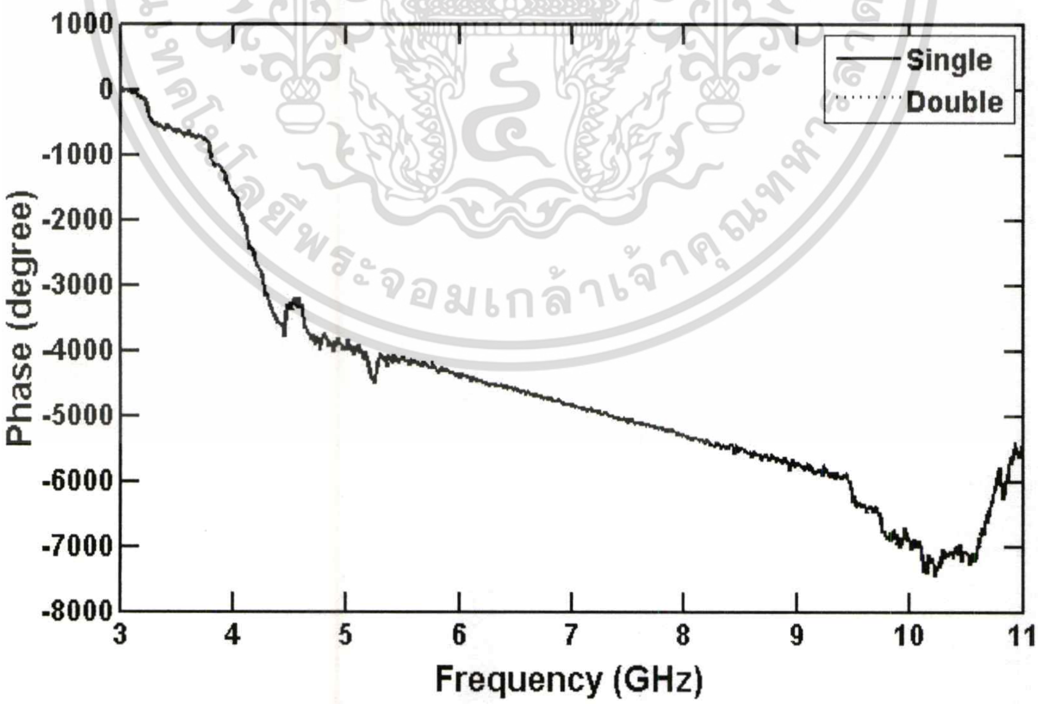

Figure 5.9 The comparisons of channel transfer function between single and double directional transmission on wrist position; phase.

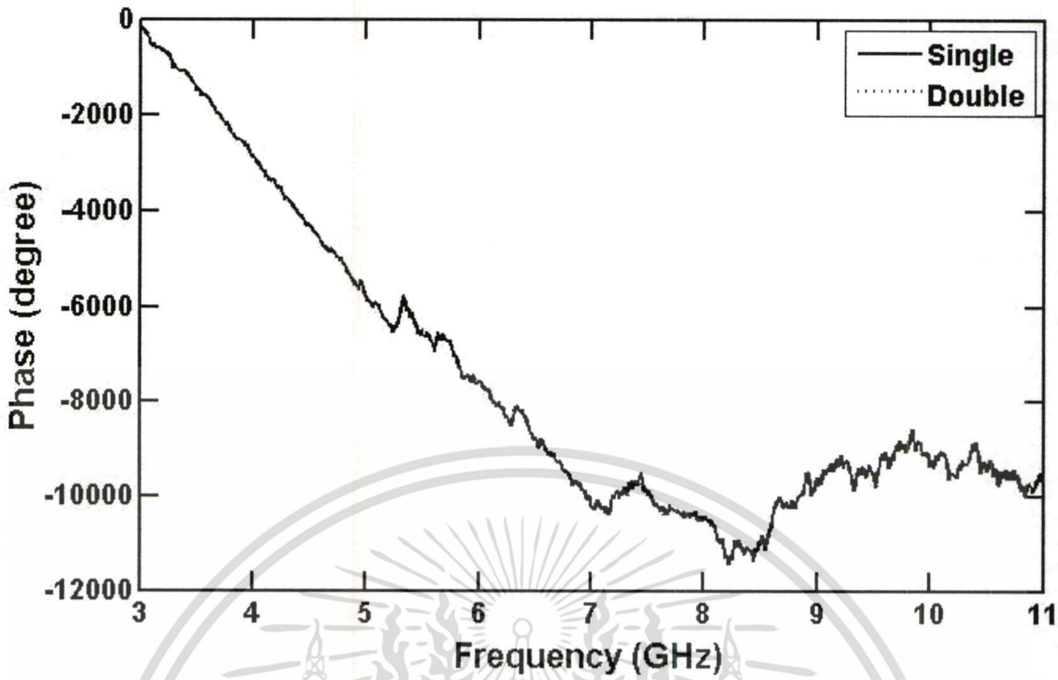

Figure 5.10 The comparisons of channel transfer function between single and double directional transmission on knee position; phase.

5.3 Path Loss of Channel Transfer Function

The path loss, which is given by the ratio between transmitted and received power is directly calculated from the measurements data, averaging over the measured frequency transfers at each frequency points, and it can be represented as a function of the distance between transmitter and receiver. Figure 5.12 shows the single waveform transmission of each position on body. For the results, we can see that path loss on chest position is the lowest and on knee position is the highest when compared with other position as shown in table 5.2. The double transmission waveform loss result shows in figure 5.13. The result on chest position is also higher than other position. For the measurement setup proposed, the antenna radiation pattern is a function which weight the path loss and the distance between the Tx and the Rx are lengthy distances. This is why for the chest position of measurements from both of single and double transmission waveform are higher. Moreover, it can know that the measuring of double transmitting antenna reduces path loss calculation is higher than a single transmitting antenna. However, the path loss is increased the effect may come from environment and human body absorption.

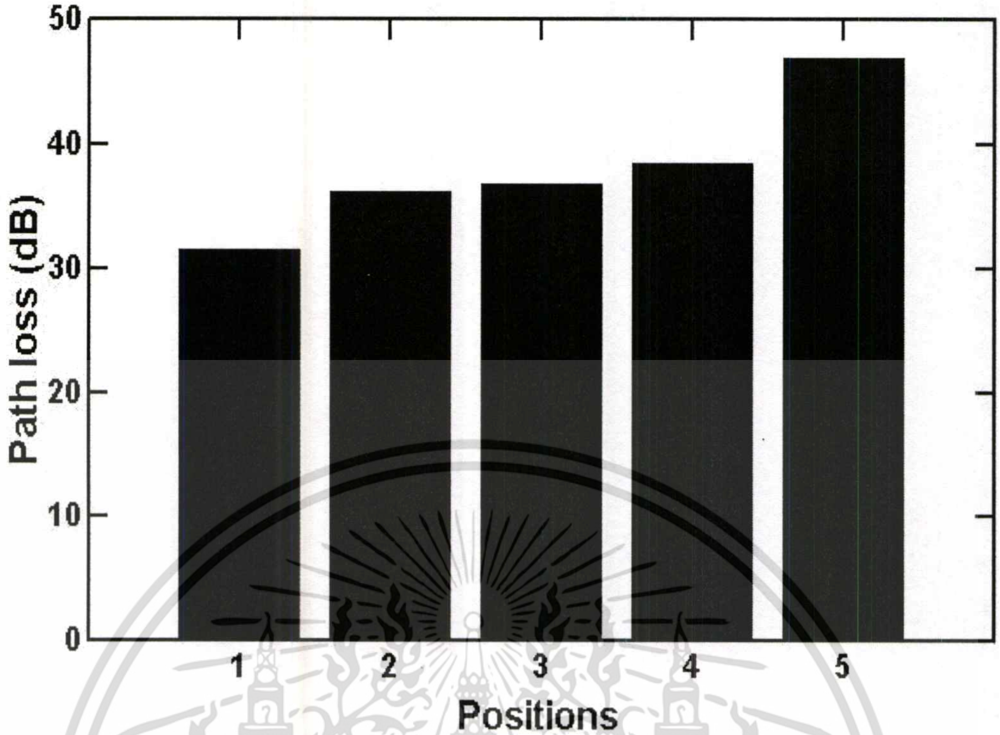

Figure 5.11 The path loss of single path loss of each position on body.

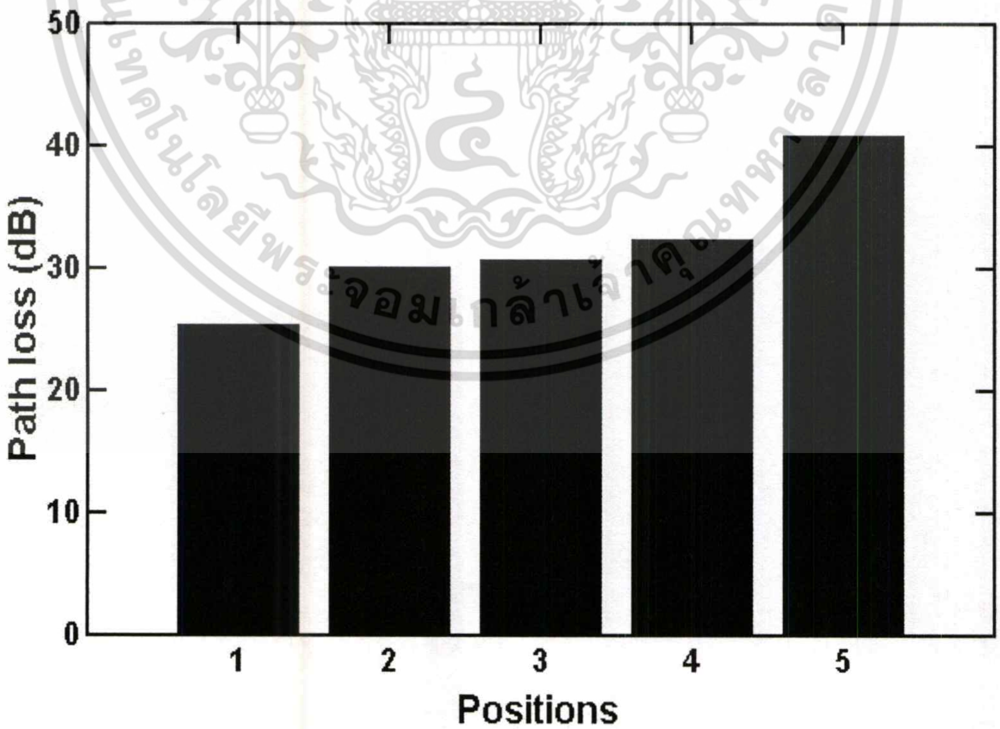

Figure 5.12 The double path loss.

Table 5.2 The single path loss and the double path loss values of each position on human body.

Position	Antenna height	Distance of Tx and Rx antenna	Single Path loss (dB)	Double Path loss (dB)	Difference (dB)
1	130 cm	30 cm	31.5	25.5	6
2	138 cm	38 cm	36.1	25.5	10.6
3	100 cm	23 cm	36.8	30.8	6
4	80 cm	20 cm	38.5	32.4	6.1
5	40 cm	60 cm	46.9	40.9	6

From table 5.2 the single path loss and the double path loss values of each position on human body. We can particularly see the path loss of each pointing as a single and double results, for the same point of a single transmitted waveform have most path loss than double transmitted waveform.

5.4 Power Delay Profile (PDP)

Power delay profile were produced by averaging all impulse responses. Figure 5.29 show the power delay profile of UWB-HB with difference positions in 3D. Which consists of the Tx and Rx antennas of each position. The figure shown that the received signal power will be greatly increased when using double transmission waveform. We can particularly see the frequency characteristic of transfer function and received power at the position 1 is highest, due to the Rx antenna is closer Tx antenna than other positions. The effect of human body shadowing on the UWB antenna propagation, signal level at each pointing down. The lowest level of the signal due to the refection on human body surface and the structure of the antenna. However, the received signal power is increased or decreased when Tx and Rx antennas are near filed.

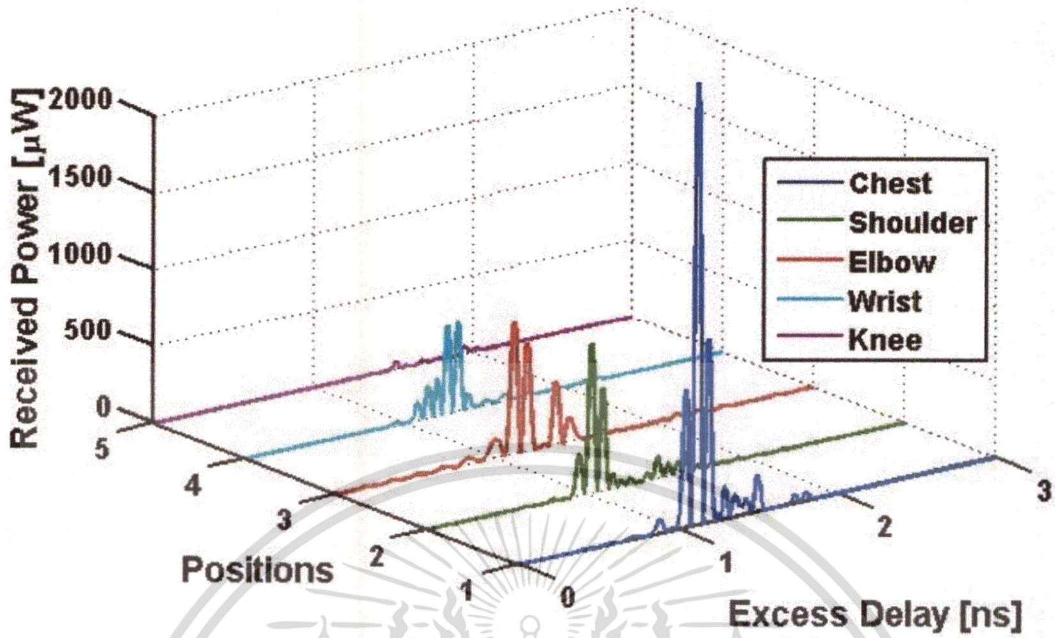

Figure 5.13 The power delay profile of UWB-HB with difference positions.

5.5 The Received Waveform of UWB-HB Transmission

5.5.1 Single and Double Received Waveform

Comparing the results of the received waveforms of UWB-HB transmission in figures 5.14 to 5.18, respectively. The received waveforms between single and double transmission waveform of 5 positions on human body are difference based on frequency characteristics. In the case of double received waveform, the peak amplitudes are higher than the peak amplitudes of single received waveform. Furthermore, the UWB-IR communication system of the double transmission waveform can be improved the received waveform than single transmission waveform.

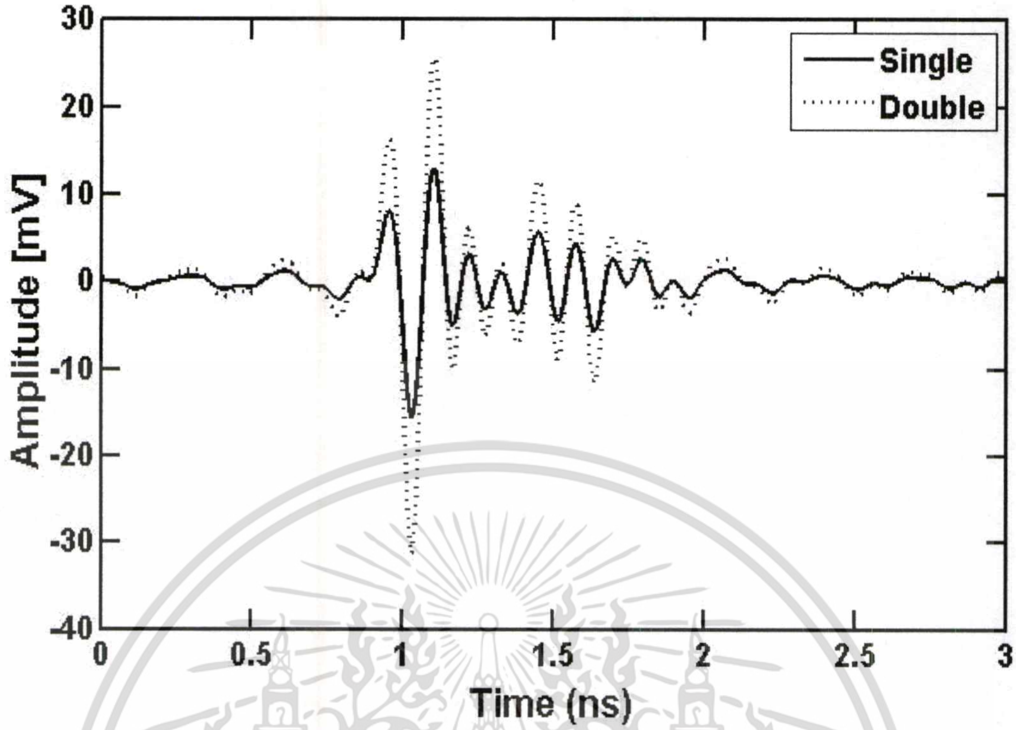

Figure 5.14 The comparisons of received waveform between single and double directional transmission on chest position.

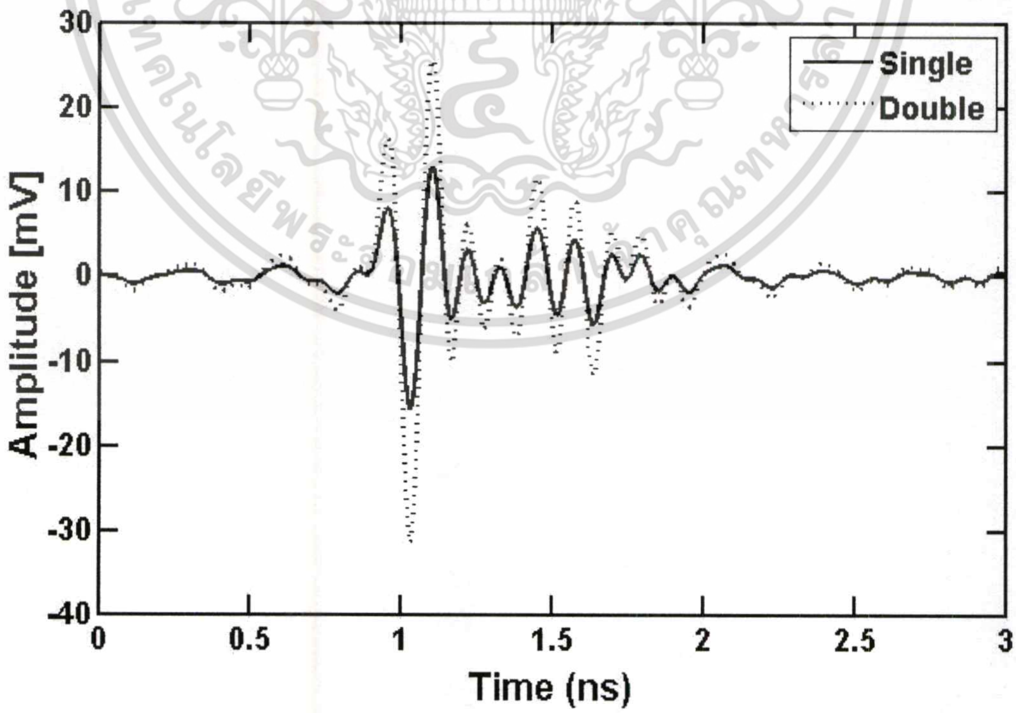

Figure 5.15 The comparisons of received waveform between single and double directional transmission on shoulder position.

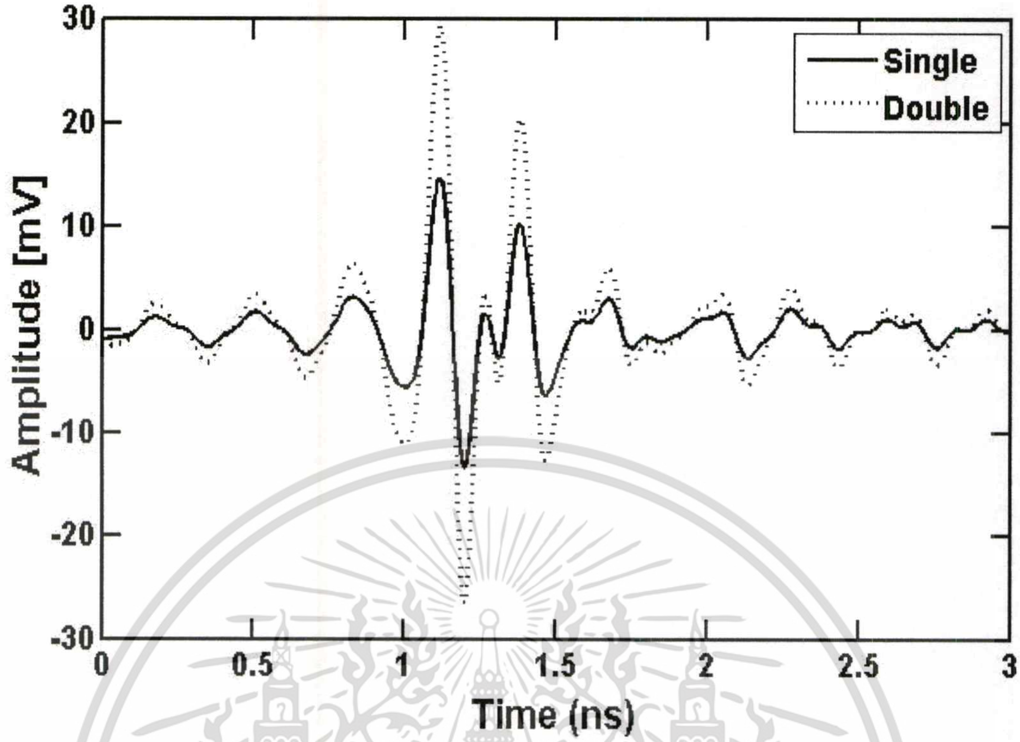

Figure 5.16 The comparisons of received waveform between single and double directional transmission on elbow position.

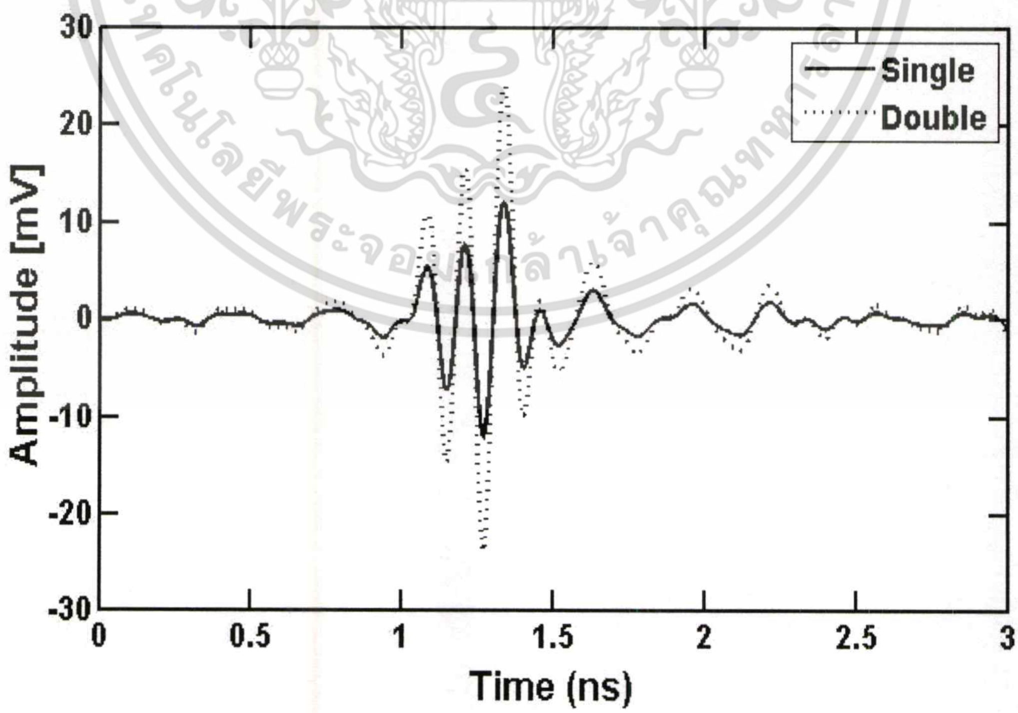

Figure 5.17 The comparisons of received waveform between single and double directional transmission on wrist position.

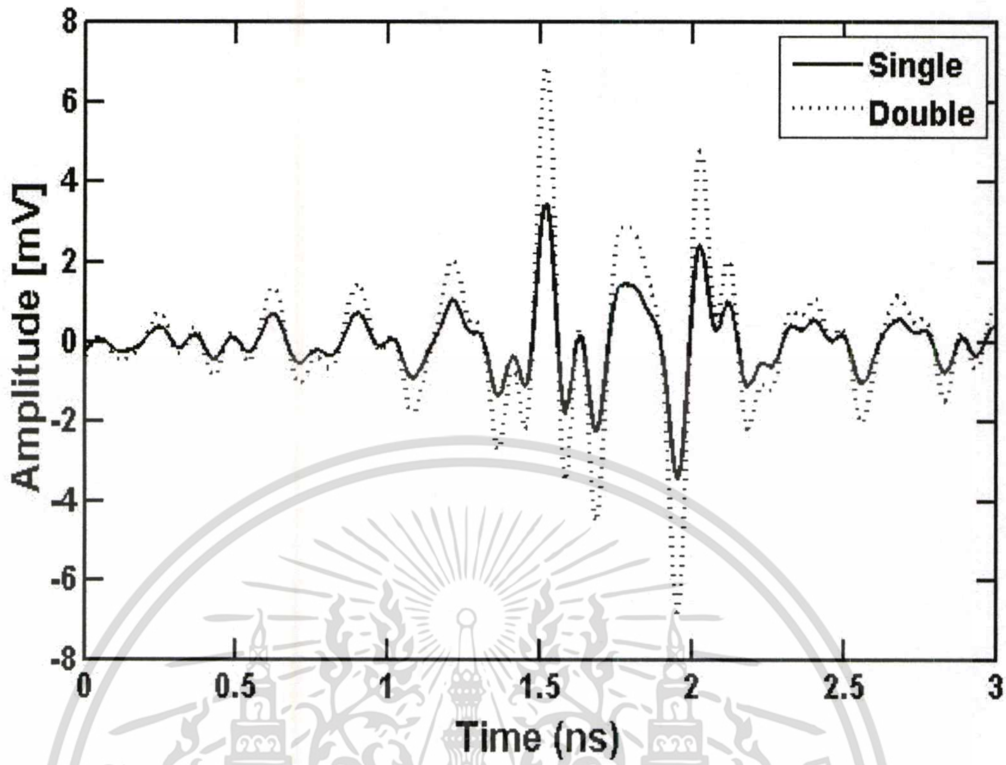

Figure 5.18 The comparisons of received waveform between single and double directional transmission on knee position.

5.5.2 Matched Filter Received Waveform

From the results of improvement by using matched filter and transmitted template. The amplitudes of the output received waveform with rectangular passband transmitted waveform satisfying the FCC spectral mask for indoor and outdoor limit is shown in figure 5.19 to 5.23. The peak power of received waveform on chest position is satisfied 61.9 mV as a highest amplitude is shown in figure 5.19. For the lowest position is satisfied 32.7 mV on knee position is shown in figure 5.23. As the figure 5.24 and 5.25 are shown the amplitudes of signal waveform at the output of matched filter when compare with without matched filter at the body positions (1 to 5). From these figures, the peak amplitudes of matched filter has less distortion compared with single and double received waveform. Because there is no effect of transmitter and receiver antennas.

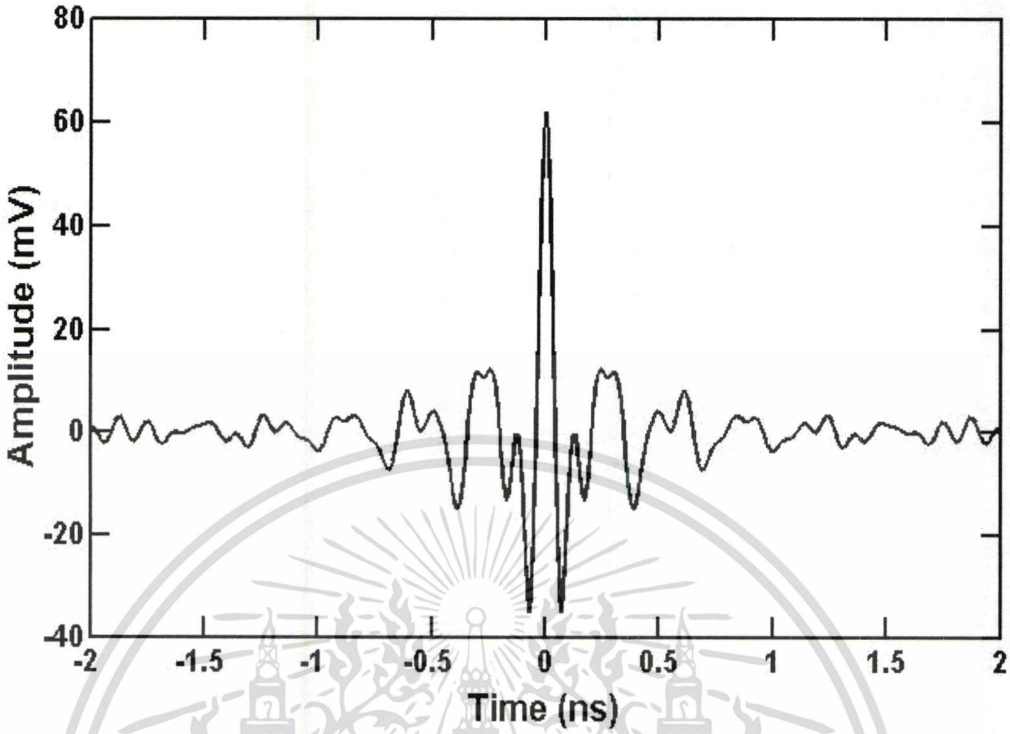

Figure 5.19 Received waveform with match filter on chest.

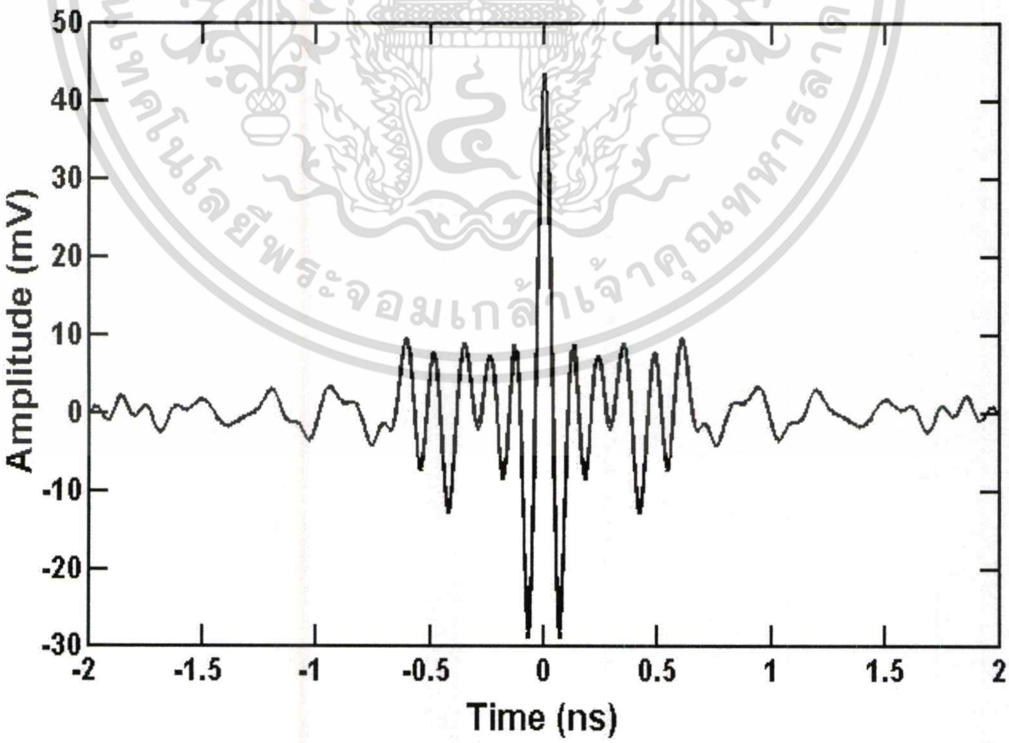

Figure 5.20 Received waveform with match filter on shoulder.

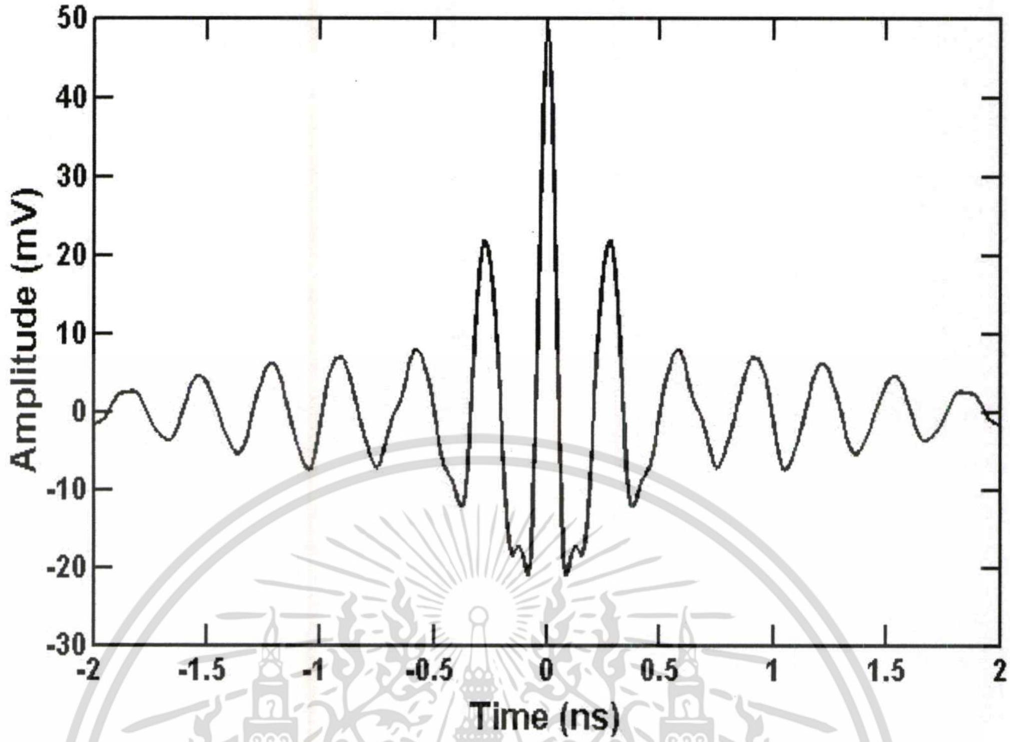

Figure 5.21 Received waveform with match filter on elbow.

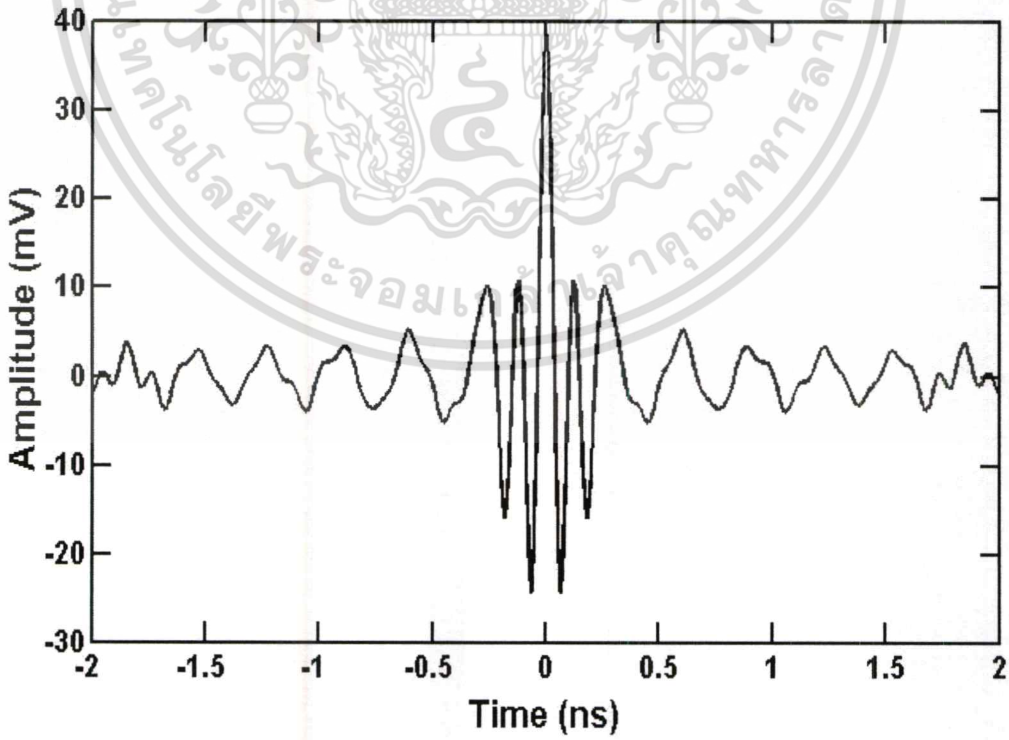

Figure 5.22 Received waveform with match filter on wrist.

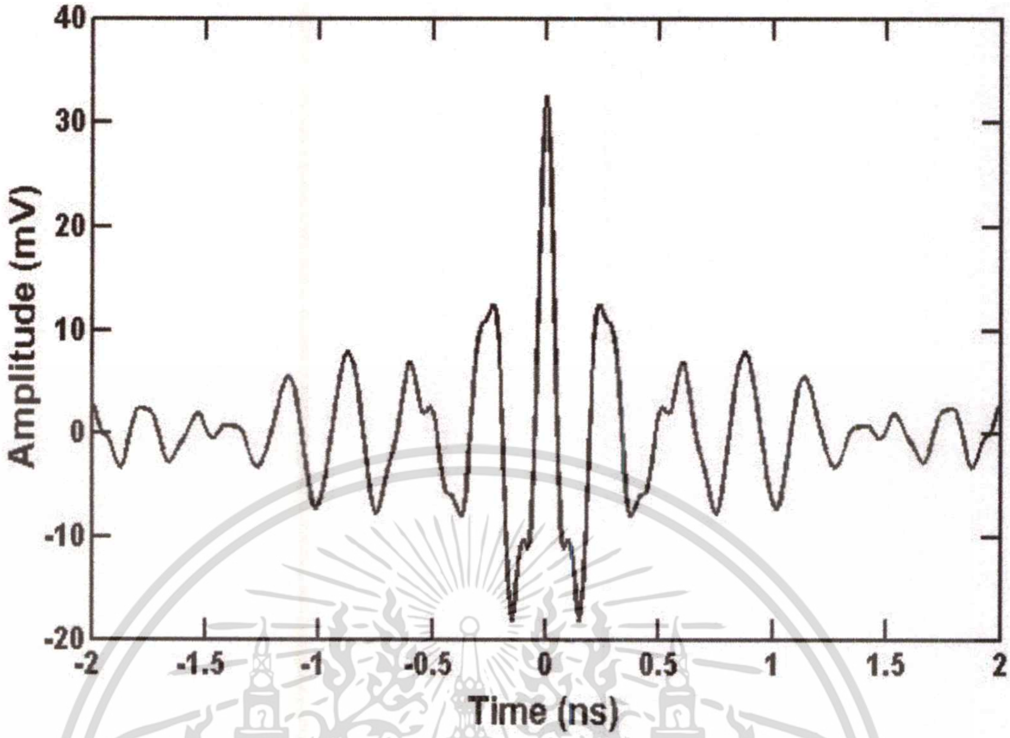

Figure 5.23 Received waveform with match filter on knee.

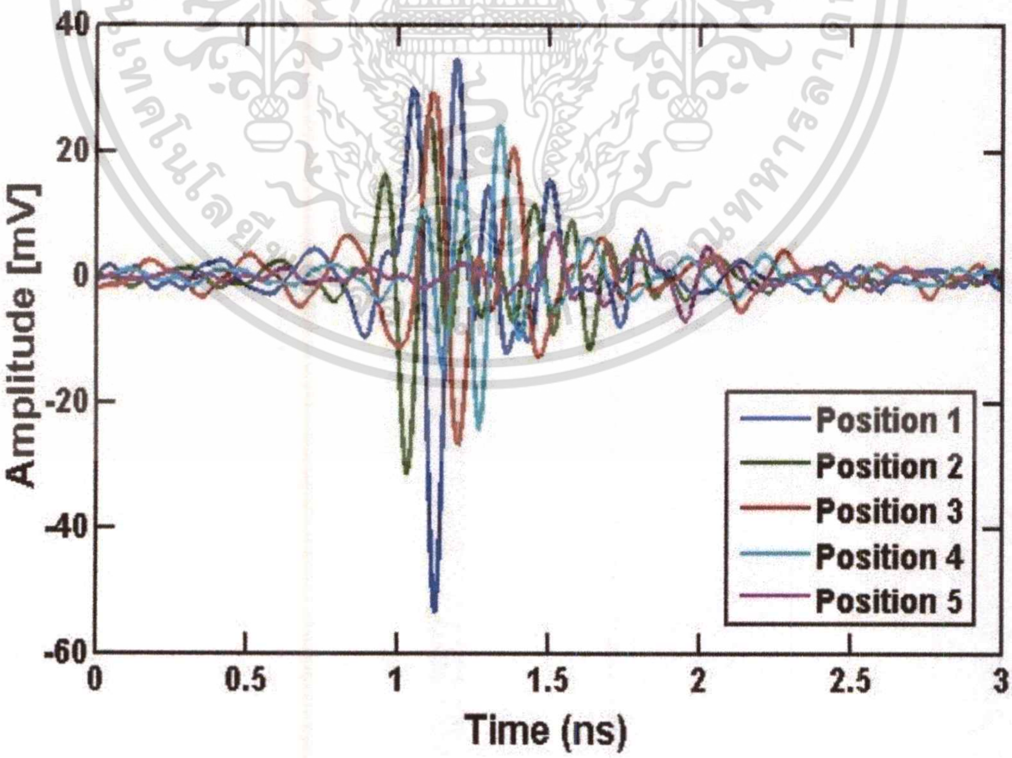

Figure 5.24 The comparisons of received waveform without matched filter on 1 to 5 position.

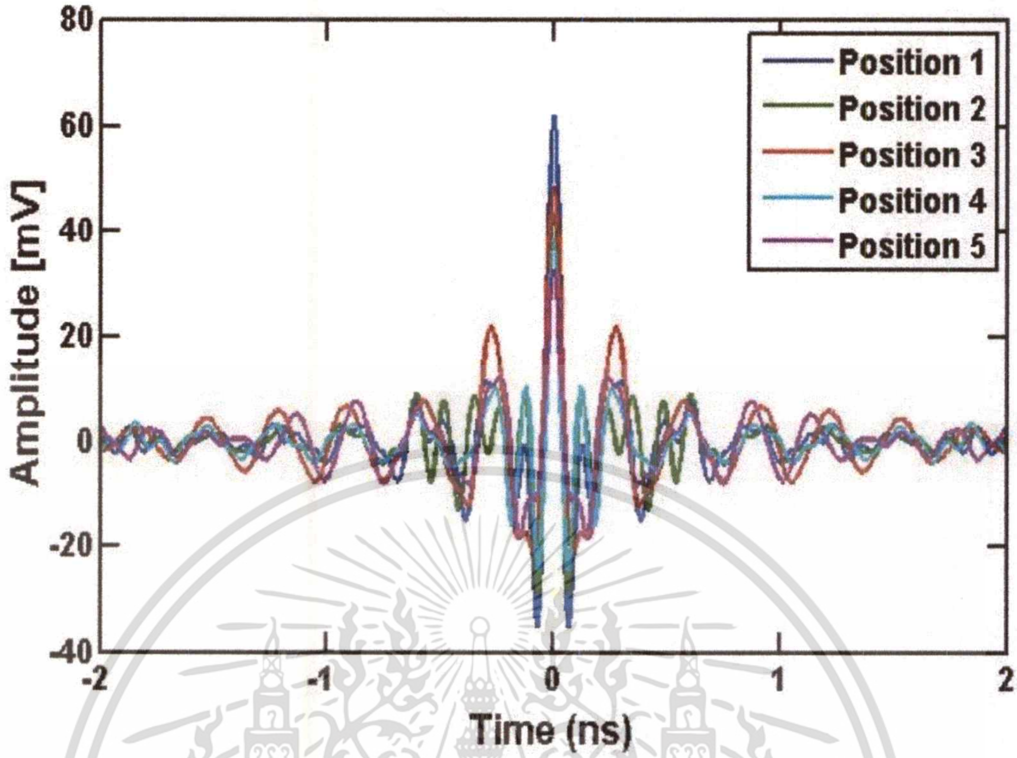

Figure 5.25 The comparisons of received waveform with matched filter on 1 to 5 position.

5.6 The Evaluation of UWB-HB Transmission Performance between Single and Double Directional Transmission on Difference Positions.

This section, evaluated the BER performance of UWB-HB transmission are shown. All of these parameters are based on the regulation of WBAN (IEEE802.15.6). The BER of UWB-HB transmission is compared between the single waveform transmitted and the double waveform transmission of each position on human body are shows in figure 5.24 to 5.28, respectively. It can be seen that the BER is accepted to 10^{-6} for UWB communication system. The BER of double transmission waveform is lower than the single transmission waveform about 6 dB of E_b/N_o. Due to the optimization of waveform distortion has been compensated by using double transmission waveform. So it can be confirmed that the performance of provided DWT is a solution to be used on WBAN transmission waveform.

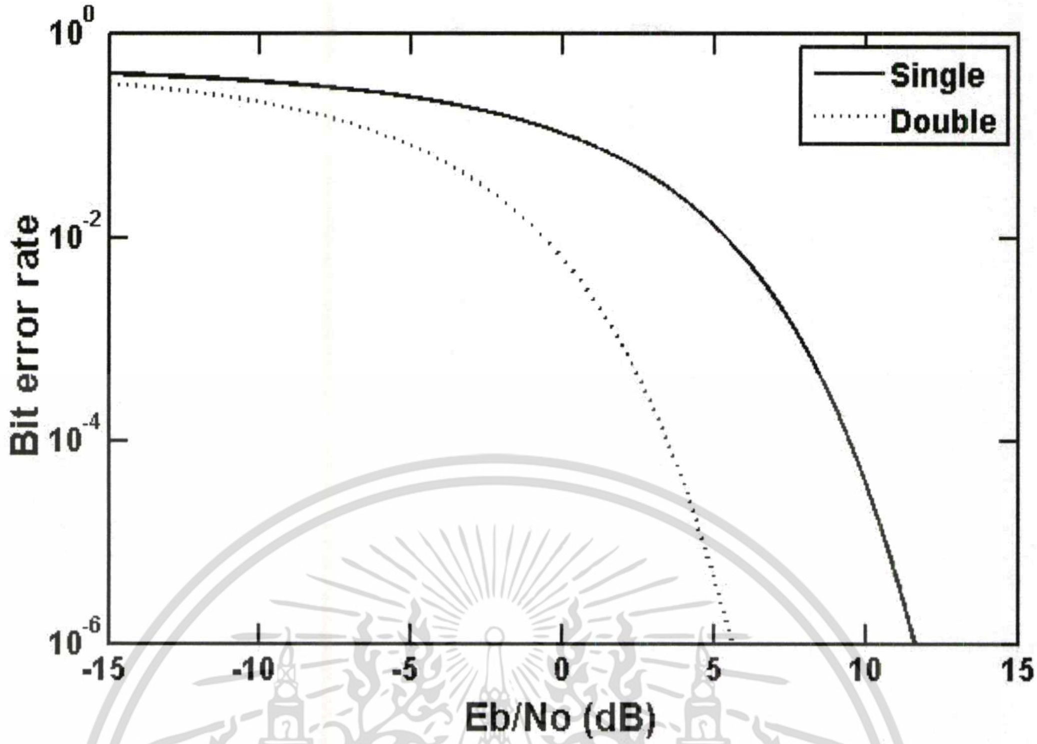

Figure 5.26 The comparison of BER between single and double directional transmission on chest position.

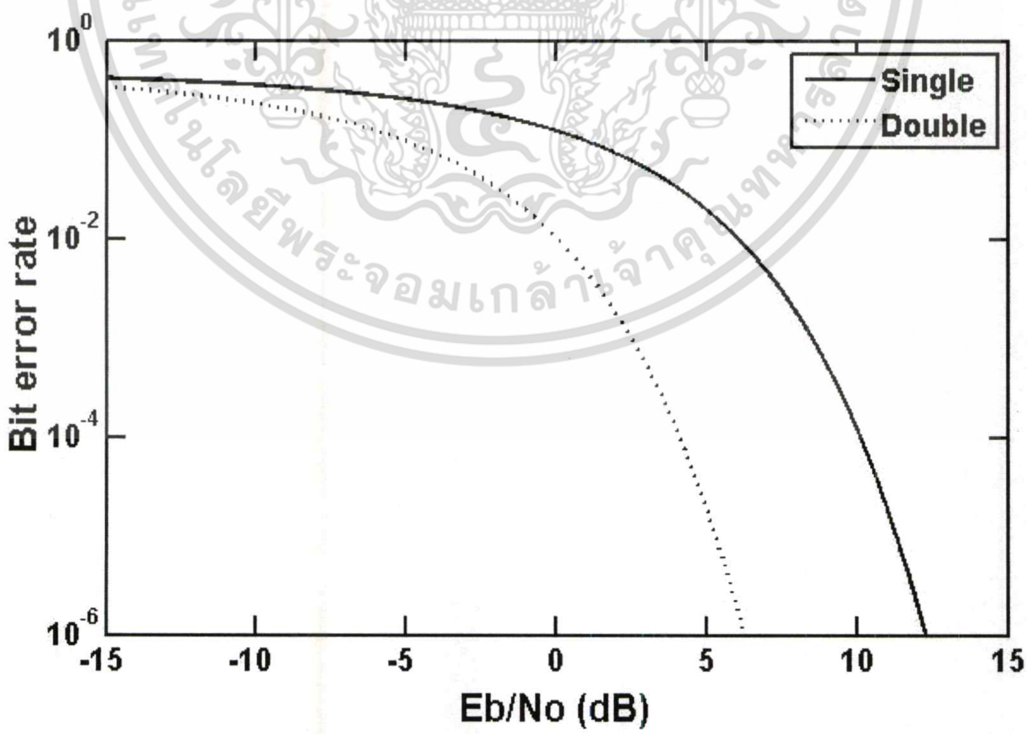

Figure 5.27 The comparison of BER between single and double directional transmission on shoulder position.

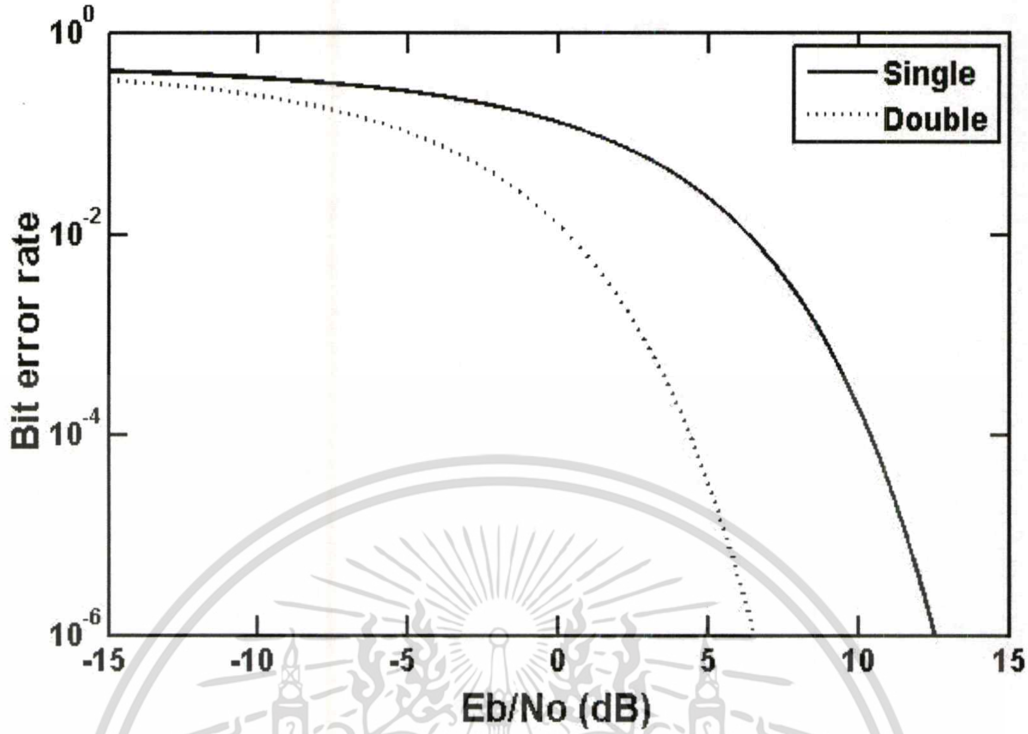

Figure 5.28 The comparison of BER between single and double directional transmission on elbow position.

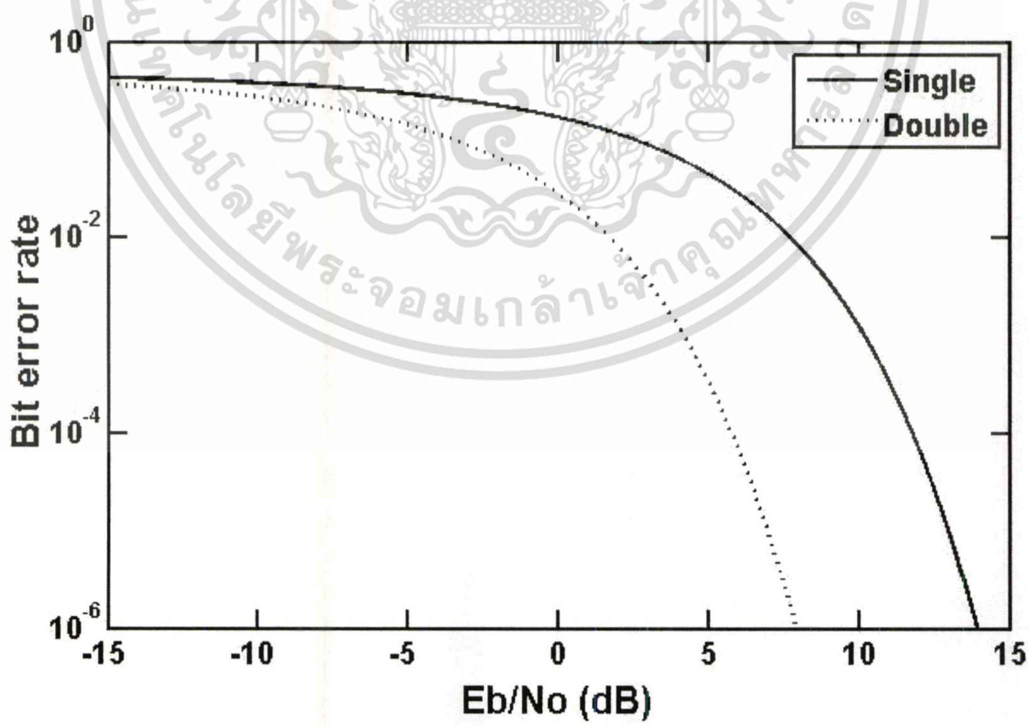

Figure 5.29 The comparison of BER between single and double directional transmission on wrist position.

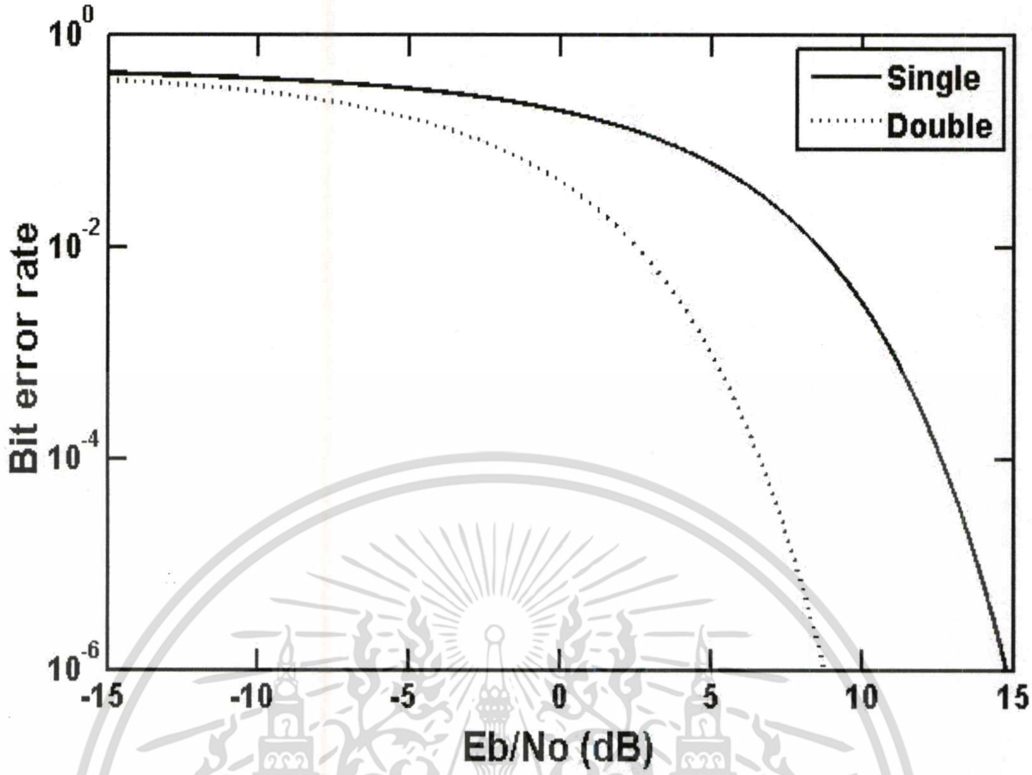

Figure 5.30 The comparison of BER between single and double directional transmission on knee position.

5.7 Summary

This chapter is shown the results base on measured data the results described above, and also presented the real results of the measurement in an indoor environment. The measurement carried out the single and double transmission waveform of each position on human body, the results of experiment are shown and compared between single and double transmission waveform of magnitude of channel transfer function, phase of channel transfer function, path loss, received waveform, matched filter received waveform, power delay profile and bit error rate. The characterization of transmission loss an indoor in UWB-IR system can be improvement by using matched filter at the receiver side, this approach is more useful to design and evaluate the UWB-IR wireless systems.

CHAPTER 6
CONCLUSIONS AND FUTURE WORKS

6.1 Conclusions

This thesis presents an experimental study of UWB-HB impulse radio transmission with double direction transmission waveform. The accuracy of the extension of Friis' transmission formula for UWB channel based on measurements is evaluated. Its applicability in the Fresnel and far-field region was also experimentally studied. The observed error in the Fresnel region is caused by the radial field. In addition, the distortion of the extended Friis' transmission formula is very low and is better than the original Friis' transmission formula both in the Fresnel and far-field regions. More comprehensive studies are necessary though, to consider the type of antennas (size and current distribution) and to find how to compensate this error. To know the individual antenna parameters, three-antenna measurement was introduced to calibrate the measurement system. Some typical UWB antennas were evaluated by using this proposed technique. The evaluation method of the UWB transmission gain link budget was presented, which includes the transmitted waveform, the antennas, free space propagation, and matched filter receiver.

A general obtained are shortly summarized. The data analysis results are that introduces the concept of measuring single and double transmission waveform by using the application of Friis' transmission formula in BAN-UWB channel systems, which is introduced the receiver matched filter to get the maximum SNR. The connectivity and propagation characteristics in BAN composed by 5 positions (chest, shoulder, elbow, wrist, and knee) at transmitters and 1 position is fixed on center (navel) of human body at a receiver. A number of measurement have been undertaken in the last few years to characterize the spatial UWB channel. In most of those studied, the objective is introduced double transmission waveform of UWB-HB in this master thesis. For realizing a reliable UWB-IR communication in WBAN, we have improved the received waveform distortion by introducing matched filter at the receiver side. The simulation and measurement results of each position on human body is investigated the performance of transmission waveform by using double waveform transmission. The both of transmitter and receiver are meander line antennas. Based on these definitions, the double waveform transmission can obviously improve performance of UWB-WBAN systems than single transmission waveform. The characterization of transmission loss an indoor in UWB-IR system can be improvement by using matched filter at the receiver side, this approach is more useful to design and evaluate the UWB-IR wireless systems.

6.2 Future Works

At the recent, many researchers are interested in the wireless communication technologies. The UWB-WBAN channel models for future measurements. We recommend to take place in expected WBAN utilization areas, such as hospital or elderly care or residential homes. Moreover, the measurements on different models i.e. when a patient sitting (as in figure 6.1) or lying on the bed (as in figure 6.2), more number of volunteers, different environments, human body movement and other body positions will influence the parameters of the models.

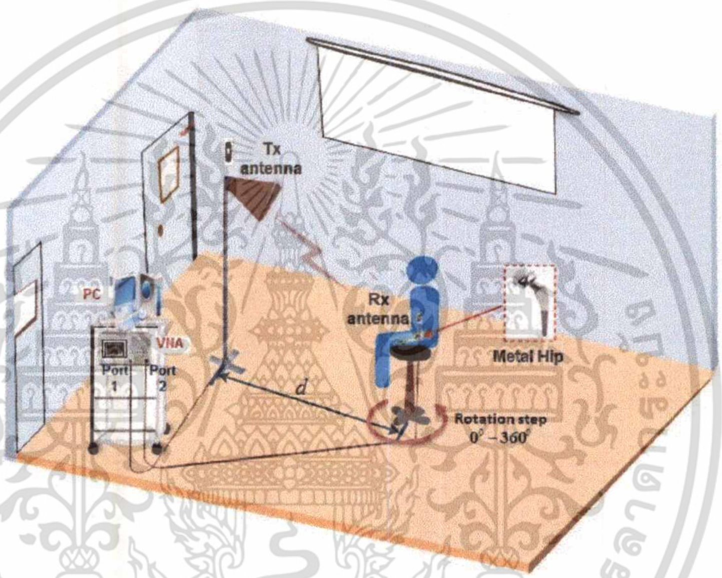

Figure 6.1 WBAN in medical application (1).

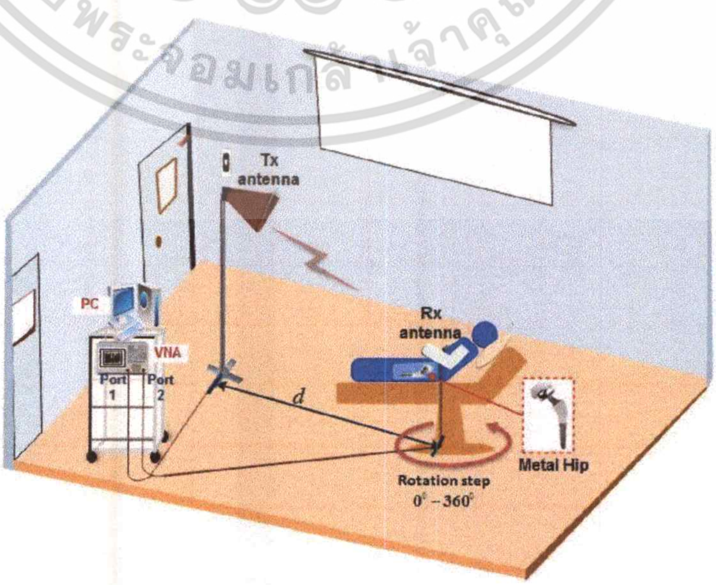

Figure 6.2 WBAN in medical application (2).

REFERENCES

[1] F. Nekoogar, "Ultra-Wideband Communications: Fundamentals and Applications," United States of America: Prentice-Hall PTR, Aug. 2005.

[2] S. Kazimierz, and M. Debra, "Ultra-Wideband Radio Technology," England: John Wiley & Sons Ltd. 2004.

[3] M. Hämäläinen, P. Pirinen, J. Iinatti, A. Taparugssanagorn, "UWB Supporting Medical ICT Applications." 2008 IEEE International Conference on Ultra-Wideband, Hannover, Germany, 2008.

[4] K. Siwiak, "Ultra-Wide Band Radio: Introducing a New Technology," 2001 Spring IEEE Vehicular Technology Conference (VTC), vol. 2, pp. 1088-1093, May 2001.

[5] K. Siwiak, "Ultra-Wide Band Radio: The emergence of an Important RF Technology," 2001 Spring IEEE Vehicular Technology Conference (VTC), vol. 2, pp. 1169-1172, May 2001.

[6] Federal Communications Commission, "Revision of Part 15 of the Commission's Rules Regarding Ultra-Wideband Transmission Systems," First Report and Order, FCC 02-48, Apr. 2002.

[7] M. Di Benedetto and G. Giancola, "Understanding Ultra Wideband Radio Fundamentals," New Jersey: Prentice Hall, 2004.

[8] H. Nekoogar and R. Prasad, "Introduction to Ultra Wideband for Wireless Communications," Springer Science, 2009.

[9] Z.N. Chen, X.H. Wu, N. Yang and M.Y.W. Chia, "Consideration for source pulse and antennas in UWB radio systems," IEEE Trans. Antennas Propagation., 52(7), pp. 1739-1748, 2004.

[10] B. M. Sadler, D. Goeckel, M. L. Honig, A. J. van der Veen and Z. Xu, "Introduction to the Issue on Performance Limits of Ultra-Wideband Systems," in IEEE Journal of Selected Topics in Signal Processing, vol. 1, no. 3, pp. 337-339, Oct. 2007.

[11] H.T. Friis, "A Note on A Simple Transmission Formula," Proceedings of IRE, vol. 34, no. 5, pp. 254–256, May. 1946.

[12] IEEE. IEEE 802.15 TG-6 Body Area Networks (BAN), 2011 [visited May 2011].

[13] Daniel Lewis (Ed). 802.15.6 call for applications - response summary. Technical report, IEEE, January 2009 [visited June 2011].

[14] Arthur Astrin (Ed.). Draft standard for body area network. Draft, IEEE P802.15 Working Group for Wireless Personal Area Networks (WPANs), May 2010 [visited June 2011].

[15] Mehmet R. Yuce, Jamil Y. Khan, Wireless body Area Network: Technology, Implement, and Applications, Pan Standford Publishing Pte. Ltd., 2012.

[16] Kazimierz Siwiak, Debra Mc. Keown, "Ultra-Wideband Radio Technology," John Wiley & Sons, Ltd, 2004. Chapter 2, pp. 30-31.

[17] "Federal communications commission (FCC), code of federal regulations (CFR), title 47 part 95, MICS band plan,'' [Online]. Available: www.fcc.gov, Mar 03, 2013.

[18] K. S. Kwak, S. Ullah and N. Ullah, "An overview of IEEE 802.15.6 standard," 2010 3rd International Symposium on Applied Sciences in Biomedical and Communication Technologies (ISABEL), pp. 1-6, 2010.

[19] A. W. ASTRIN, H.-B. LI, and R. KOHNO, "standardization for body area networks," IEICE Transactions on Communications, vol. E92.B, no. 2, pp. 366.372, 2009.

[20] A. Mehaoua, "Wireless Body Area Networks for HealthCare," SIECPC 2013 Workshop on Pervasive HealthCare, Apr. 27, 2013.

[21] B. Zhen, H. B. Li, and R. Kohno, "IEEE body area net-works and medical implant communications," Proceed-ings of the ICST 3rd International Conference on Body Area Networks, Tempe, Arizona, 2008.

[22] B. Zhen, M. Patel, S.-H. Lee, and E.-T. Won, "Body area network (BAN) technical requirements," 15-08-0037-03-0006-ieee-802-15-6-technical-requirements document-v-5-0.doc

[23] S. Ullah et al, "A Review of Wireless Body Area Networks for Medical Applications," International J. of Communications Network and System Sciences (IJCNS), vol. 2, no. 8: 797-803. July 27, 2009.

[24] Federal Communication Commissio, "Revision ofpart 15 ofthe commission's rules regarding UWB Transmission Systems," First Report, FCC 02-48,Apr.2002.

[25] ESTI, "ECC Hamaminished Standards Covering Ultra Wideband (UWB) Applications." Standisation Mandate: DG ENTR/G/3M/329, Brussels, Feb. 2003.

[26] ETSI, "ECC Decision of 24 Mach 2006 on the Harmonish Conditions for Devices Using UWB technologies in band below 110.6 GHz," Doc. ECC/DEC/(06)04, Mar.2006.

[27] W. Hirt and M. Weisenhornk, "Overview and Implications of the Emerging Global UWB Radio Regulatory Framework," 2006 IEEE International Conference on Ultra-Wideband, Waltham, MA, pp. 581-586, 2006.

[28] M. P. Wylie-Green, P. A. Ranta and J. Salokannel, "Multi-band OFDM UWB solution for IEEE 802.15.3a WPANs," IEEE/Sarnoff Symposium on Advances in Wired and Wireless Communication, 2005., Princeton, NJ, pp. 102-105, 2005.

[29] N. Salman, I. Rasool and A. H. Kemp, "Overview of the IEEE 802.15.4 standards family for Low Rate Wireless Personal Area Networks," Wireless Communication Systems (ISWCS), 2010 7th International Symposium on, York, pp. 701-705, 2010.

[31] S. Promwong, W. Hachitani and J. Takada, "Experimental Evaloation Scheme of UWB Antenna Performance," Technical Meeting on Instrument and Measurement, IEE Japan, IM-03-35, June. 2003.

[32] S. Promwong, W. Hachitani, J. Takada, P. Supanakoon and P.Tangtisanon, "Experimental Study of Ultra-Wideband Transmission Based on Friis' Transmission Formula," The Third International Symposium on Communications and Information Technology (ISCIT) 2003, vol. 1, pp. 467-470, Sept. 2003.

[33] P. Supanakoon, K. Teplee, S. Promwong, S. Keawmechai and J. Takada, "Theoretical SNR Gain and BER Performances of UWB Communications with Matched Filter and Correlation Receivers," The International Technical Conference on Circuits/Systems, Computers and Communications (ITC-CSCC 2006), no. 3, pp. 269-272, July 2006.

[34] A. Technologies." Agilent technologies 8510C network Analyzer System," 3rd Edition, USA, May, 2001.

[35] Skycross Company, "3.1-10 GHz Ultra-Wideband Antenna for Commercial UWB Applications." [Online]. Available: http://www.skycross.com/. 2003.

[36] P. Supanakoon, K. Wansiang, S. Promwong and J. Takada, "Simple Waveforms for UWB Communication," ECTI International Conference, pp. 626-629, May 2005.

BIOGRAPHY

PERSONAL INFORMATION

Name:	Ms. Phouthong Southisombath
Date of Birth:	February 2^{nd}, 1993
Born:	Vientiane, Laos
Nationality:	Lao
Current Address:	Lao-Thai Rd, Sokpaluang, Vientiane, Laos
E-mail:	tity_sout@hotmail.com

EDUCATIONS

Bachelor Degree

Thesis	Code Division Multiple Access (CDMA)
Major:	Telecommunications Engineering
Year:	2009-2014
Department:	Electronic and Telecommunications Engineering
University:	National University of Laos (NUOL)

Master Degree

Major:	Computing in Engineering Systems
Year:	2014-2016
Laboratory:	Ultra Wideband-Impulse Radio Laboratory, Department of Telecommunications Engineering, Faculty of Engineering
College:	International College
University:	King Mongkut's Institute of Technology Ladkrabang (KMITL), Bangkok, Thailand

Research Interests

Ultra Wideband (UWB), Wireless Body Area Network (WBAN)

LIST OF PUBLICATIONS

1. P. Southisombath, S. Promwong, K. Southisombath, “A Path Loss Model on Body for BAN-UWB,” The 1st AUN/SEED-Net Regional Conference for Computer and Information Engineering (RCCIE 2015), Hanoi, Vietnam, 1-2 October 2015, ISS-04, pp. 140-143.
2. P. Southisombath, K. Southisombath and S. Promwong, “Computational Analysis of Waveform Distortion for Ultra Wideband Impluse Radio Transmission,” The 34th JSST Annual Conference International Conference on Simulation Technology (JSST2015), Toyama, Japan, 12-14 October 2016.

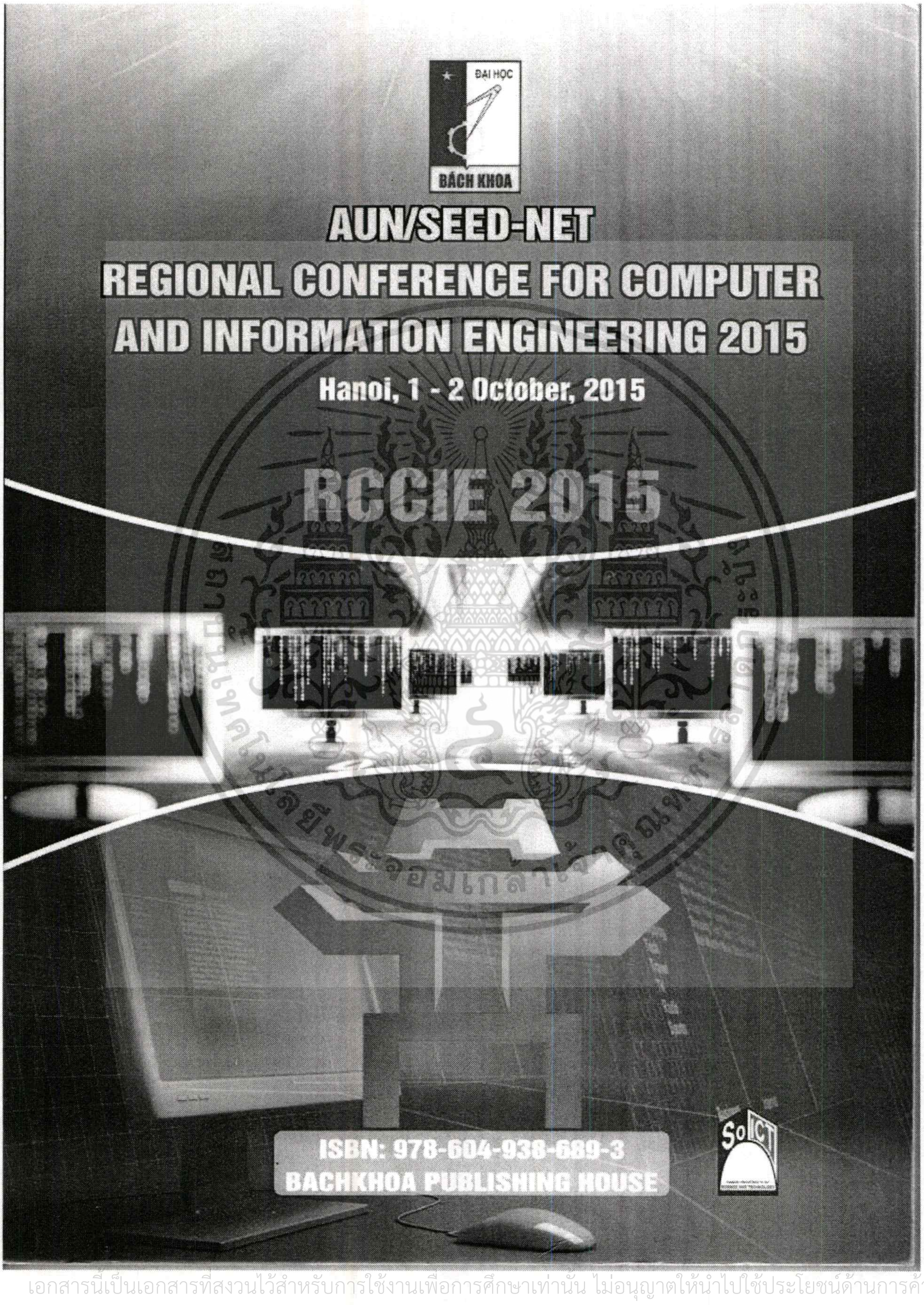
ĐẠI HỌC
BÁCH KHOA
AUN/SEED-NET
REGIONAL CONFERENCE FOR COMPUTER AND INFORMATION ENGINEERING 2015
Hanoi, 1 - 2 October, 2015
RCCIE 2015
ISBN: 978-604-938-689-3
BACHKHOA PUBLISHING HOUSE
SoICT

A Path Loss Model on Body for BAN-UWB

Phouthong Southisombath[1], Sathaporn Promwong[2], Khamphoui Southisombath[3]
[1] *International Collage*
[2] *Department of Telecommunication Engineering, Faculty of Engineering*
King Mongkut's Institute of Technology Ladkrabang, Bangkok 10520, THAILAND
[3] *Department of Electronic and Telecommunication, Faculty of Engineering, National University of Lao, LAOS*

Abstract

This paper presents a path loss models for body area network ultra wideband (BAN-UWB) with different body mass index (BMI). The rectangular passband waveform is used as transmitted waveform. The body transfer functions are measured by using vector network analyzer (VNA) at frequency ranging from 7.25 GHz to 8.5 GHz. The path losses based on average and peak power losses are evaluated. The linear regression model is used to characterize the path loss parameters. This technique is useful as the basis for designing the evaluation of UWB systems and WBAN.

Keywords— UWB, BAN, WBAN, path loss, impulse radio

1. Introduction

Big frequency band of wireless technology is UWB technology that new idea for body area network. The UWB are low power and high speed. BAN-UWB is a promising new application because of its potentiality in different works such as health, sport, monitoring, multimedia, surveillance, entertainment and data transfer [1]. In addition, the channel model including antenna is necessary for BAN-UWB [2]. There are some researches that model the BAN-UWB channels such as [3, 4]. However, there are no research that considers the effect of body mass index (BMI).

This paper, evaluated path loss models of BAN-UWB. The rectangular passband waveform is used as transmitted signal. The on-body channel transfer functions were measured using vector network analyzer (VNA) frequency ranging from 7.25 GHz to 8.5 GHz. The meander line miniature antennas were used as transmitter (Tx) and receiver (Rx) antennas. The path losses based on average and peak power losses are evaluated. The linear regres sion model is used to characterize the channel parameters. The 8 sample bodies with 10 positions of each body were considered. The effect of BMI is considered.

2. BAN-UWB analysis

2.1. Transmitted wavform of BAN-UWB system

The rectangular passband waveform used for BAN-UWB system, the expressions of this waveform in time domain v_t and its spectral density Vt are [5]

$$v_t(t)=\frac{1}{f_b}\left[f_H \operatorname{sinc}(2f_H t)-f_L \operatorname{sinc}(2f_{Lt})\right] \quad (1)$$

$$V_t(f)=\begin{cases}\frac{1}{2f_b} & \left||f|-f_c\right|\le\frac{f_b}{2}\\ 0 & \left||f|-f_c\right|>\frac{f_b}{2}\end{cases} \quad (2)$$

where t is the time, f is the frequency, f_c is the center frequency, f_b is the spectral bandwidth, $f_L=f_c-f_b/2$ is the lowest frequency, $f_H=f_c+f_b/2$ is the highest frequency and function $\operatorname{sinc}(x)=\sin(\pi x)/(\pi x)$.

2.2. Receive waveform of BAN-UWB

The power spectral density (PSD) of received waveform V_r is calculated by using multiplication between channel transfer function $H_c=(f,d)$ obtained from measurement and spectral density of transmitted waveform V_t

$$V_r(f)=H_c(f,d)V_t(f) \quad (3)$$

The received waveform in time domain v_r is calculated by using inverse Fourier transform of its spectral density and it can be written as

$$v_r(t)=\mathcal{F}^{-1}\{V_r(f)\}=\int_{-\infty}^{\infty}V_r(f)e^{j2\pi ft}dt \quad (4)$$

* Corresponding author: Tel.: (+66) 971-581-819
Email: tity_sout@hotmail.com

2.3. Path loss model

For UWB-WBAN, there are two definitions of path losses: based on average and peak power losses. The path loss based on average power loss PL_a in dB is defined as the ratio between the average power of transmitted and received

$$PL_a\left[dB\right] = 10\log\left[\frac{\int_{-\infty}^{\infty}\left|V_t(f)\right|^2 df}{\int_{-\infty}^{\infty} V_r(f)^2 df}\right] \quad (5)$$

The path loss based on peak power loss PL_p in dB is defined as the ratio between the peak power of transmitted and received waveforms in time domain and it can be written as

$$PL_p\left[dB\right] = 10\log\left\{\left[\frac{\max\left[v_t^2(t)\right]}{\max\left[v_r^2(t)\right]}\right]\right\} \quad (6)$$

Linear regression is used to model the path loss. The average path loss $\overline{PL}$ in dB expressed as [6- 9]

$$\overline{PL}(d)\left[dB\right] = \overline{PL}(d_0)\left[dB\right] + 10n\log\left(\frac{d}{d_0}\right) \quad (7)$$

where d_0 is the reference distance, d is distance between Tx and Rx antennas, n is the path loss exponent which indicates the rate at which the path loss increases with distance between Tx and Rx antennas. The parameters n and $\overline{PL}(d_0)$ are evaluated by using least square method of linear regression model between parameter $\overline{PL}$ and $\log(d)$ and determine d_0 = 1 meter.

3. BAN-UWB measurement system

The body transfer function was measured by using VNA frequency ranging from 7.25 GHz to 8.5 GHz. The meander line miniature antennas were used as Tx and Rx antennas. The 8 sample bodies with 10 positions of each body were considered. The position on each body is shown in Figure 1. The parameters of measurement are list in Table 1.

The men and women bodies were measured and classified by using BMI into three body types, which are thin and fat. The BMI values of men and women are listed in Tables 2 and 3, respectively. The path losses based on average and peak power losses are evaluated and modeled.

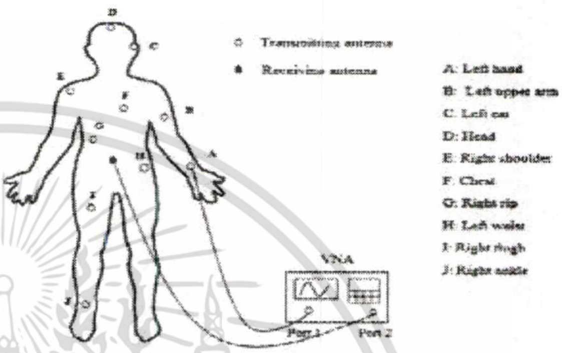

Fig.1 Measurement Setup

Table 1. Parameter of Eperiments

Parameter	Value
Frequency range	7.25 GHz to 8.5 GHz
Number of points	801
T_x and R_x antennas	Meander line
Number of samples	4

Table 2. BMI values of men cases

Body cases	Height (cm)	Weight (kg)	BMI	Body type
Thin	173	53	17.7	Thin
	179	58.5	18.3	Thin
Fat	165	80	29.4	Fat
	170	80	27.7	Fat

Table 3. BMI values of women cases

Body cases	Height (cm)	Weight (kg)	BMI	Body type
Thin	164	49	18.2	Thin
	168	43	15.2	Thin
Fat	155	58	24.1	Fat
	149	50	27.7	Fat

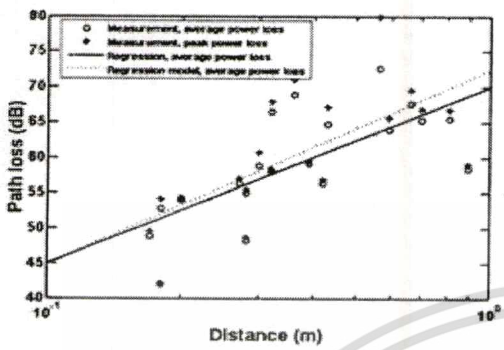

Fig 2. Path loss of thin man cases

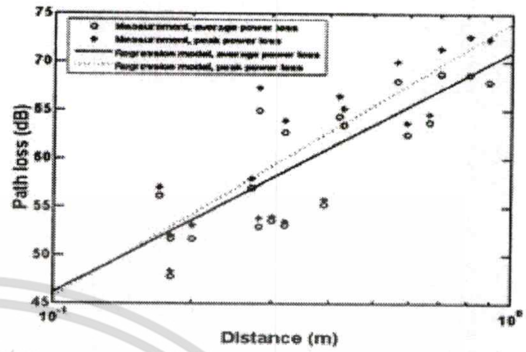

Fig 4. Path loss of thin woman cases

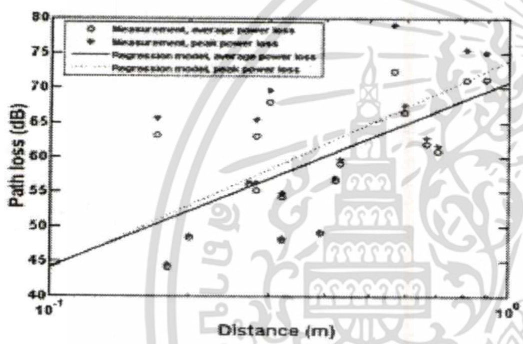

Fig. 3. Path loss of fat man cases

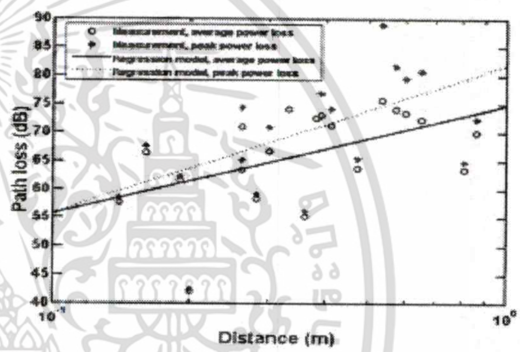

Fig. 5. Path loss of fat woman cases

4. Result and discussion

In this section, the BAN-UWB channel with linear regression models of path loss based on both average and peak power losses are evaluated and shown. Figures 2 and 3 shows the path loss models of thin and fat men, respectively. The average differences between path losses based on average and peak power losses are about 1.37 dB and 3.98 dB, respectively. The difference between theses path losses indicates the waveform distortion. Therefore, the distortion of thin is lower than fat man.

The path loss models of thin and fat women are shown in Figures 4 and 5, respectively. The average differences between path losses based on average and peak power losses are about 1.62 dB and 1.52 dB, respectively. These results reflect that the fat women has lower distortion than thin woman. Different as the man case. In this case, the distortion of thin and fat bodies has no much difference. Except the fat men, it has significant high distortion.

For the parameters of BAN-UWB channel, the path loss at referent distance (1 m) of men and women are shown in Tables 4 and 5, respectively.

Table 4. Path loss at referent distance of men cases

Body cases	Average	peak
Thin	70.03	72.45
Fat	74.83	81.84

Table 5. Path loss at referent distance of woman cases

Body cases	Average	Peak
Thin	70.90	73.93
Fat	71.00	74.03

Tables 6 and 7 list the path loss exponents of men and women respectively. Same as the path loss at referent distance, the path loss exponents of men bodies is lower than women cases.

Table 6. Path loss exponent of men cases

Body cases	Average	Peak
Thin	2.50	2.74
Fat	1.90	2.59

Table 7. Path loss exponent of women cases

Body cases	Average	Peak
Thin	2.67	2.99
Fat	2.48	2.83

5. Conclusion

This paper presents path loss models for BAN-UWB with different BMI. The thin and fat bodies are considered for both men and women cases. The results show that the thin man bodies have lower than fat bodies loss, and the fat woman bodies have a little lower loss than thin woman, path loss at referent distance and path loss exponent. The different effects between men and women bodies are not significant. For the future work, we will consider the number of people in the measurement will increase so that results are more reliable and BAN-UWB localization.

Acknowledgments

In this work, we would like to thanks AUN-SEED-Net program for the financial support to study at King Mongkut's Institute of Technology Ladkrabang (KMITL) and also our participants in this research. Moreover, we really grateful to have members of Ultrawideband Radio System (UWBRS) for help.

References

[1] M. R. Yuce and J. Khan, "Wireless Body Area Networks: Technology, Implementation, and Applications," Pan Stanford Publishing, Dec. 2011.

[2] J. Takada, T. Aoyagi, K. Takizawa, N. Katayama, T. Kobayashi, K. Y. Yazdandoost, H. Li and R. Kohno "Static Propagation and Channel Models in Body Area," COST 2100 TD(08)639, Oct. 2008.

[3] J.-M. Choi, H.-J. Kang and Y.-S. Choi, "A Study on The Wireless Body Area Network Applications and Channel Models," 2008 Second International Conference on Future Generation Communication and Networking (FGCN), pp. 263-266, 2008.

[4] K. Takizawa, T. Aoyagi and R. Kohno, "Channel Modeling and Performance Evaluation on UWB-based Wireless Body Area Networks," IEEE International Con- ference on Communications (ICC), pp. 1-5, 2009.

[5] P. Supanakoon, K. Wansiang, S. Promwong and J. Takada, "Simple Waveforms for UWB Communication," ECTI International Conference, pp. 626-629, May 2005.

[6] Leon W.Couch 2, Digital and Analog Communication Systems, Sixth Edition, 2002.

[7] T.S Rappaport, "Wireless Communication – Principles and Practices," Practice Hall, Second Edition, 2002.

[8] A. Fort, J. Ryckaert, C. Desset, P. De Doncker, P. Wambacq and L.Van Biesen, "Ultrawide-band channel model for communication around the human body," IEEE Journal on Selected Areas in Communications, vol. 24, pp. 927-933, April 2006.

[9] E. Reusens, W. Joseph, G. Vermeeren and L. Martens, "On-body measurements and character-ization of wireless communication channel for arm and torso of human," International Workshop on Wearable and Implantable Body Sensor Network, BSN07, Achen, pp. 26- 28, March 2007.

JSST 2015

The 34th JSST Annual Conference: International Conference on Simulation Technology

Toyama International Conference Center
October 12 – 14, 2015

Computational Analysis of Waveform Distortion for Ultra Wideband Impulse Radio Transmission

Phouthong Southisombath[1], Khamphoui Southisombath[2], and Sathaporn Promwong[3]

[1] International College, King Mongkut's Institute of Technology Ladkrabang
[2] Department of Electronic and Telecommunication, National University of Laos
[3] Department of Telecommunication Engineering, Faculty of Engineering, King Mongkut's Institute of Technology Ladkrabang, Bangkok 10520, Thailand.

*s7610018@kmitl.ac.th, kphoui@etllao.com, kspichay@kmitl.ac.th

Abstract. The waveform distortion in an ultra wideband impulse radio (UWB-IR) transmission can be extremely distorted through a channel transfer function even for free-space transmission because of antenna dispersion. Therefore, the understand of antenna characteristics, which effects on waveform distortion, is necessary. This paper presents the waveform distortion analysis for UWB-IR transmission and wireless body area network (WBAN) applications based on measurement data. The reciever template waveform is considered at the receiver side to maximize the SNR. In this results are evaluate based on the extended Friis' transmission formula. This technique gives very accurate results and is very useful for evaluation of UWB-IR and WBAN.

Keywords: Waveform Distortion, Impulse radio, UWB, WBAN, Friis's transmission formula

1. Introduction

The distortion of the signal in the frequency domain causes the distortion of the transmitting pulse shape. Consequently this will increase the complexity of the detection mechanism at the receiver. However, the channel in line of sight (LOS), Friis' transmission formula cannot be directly applied to the UWB radio as the bandwidth of the pulse is extremely wide. Furthermore, simple comparison between waveforms of transmitter and receiver is not significant because of the distortion of the waveform caused by the frequency response of the antenna.

In this paper, the computational scheme in free space for UWB-IR. This scheme is based on the Friis' transmission formula, adapted for UWB, in the sense that we would like to derive the equivalent antenna gain for UWB-IR systems. The transmission waveform and the receiver template waveform are keys for The extension of the Friis' transmission formula to UWB system.

2. Computational Analysis of Waveform Distortion

In communication systems, the link budget of the free space propagation loss is usually estimated by using Friis' transmission formula [1]. This formula is expressed as a function of the frequency. Moreover, the waveform may be distorted due to the frequency characteristics of the antenna.

The Friis' transmission formula has been widely used, and can be applied to the calculation of these LOS channels.

The Friis' transmission formula shall be extended to take into account the transmission signal waveform and its distortion as well [2].

Input signal $v_1(t)$ at the transmitter port is expressed as the convolution of an impulse input and the pulse shaping filter $h_1(t)$ as

$$v_1(t) = E_1\delta(t) * h_1(t), \tag{1}$$

where

$$\int_{-\infty}^{\infty} h_1^2(t)\mathrm{d}t = \int_{-\infty}^{\infty} |H_1(f)|^2\,\mathrm{d}f = 1. \tag{2}$$

Friis' formula is extended taking into account the transmission waveform as

$$H_{\text{e-Friis}}(f) = \frac{V_{\text{r}}(f)}{E_{\text{i}}} = H_{\text{f}} H_{\text{i}} \mathbf{H}_{\text{r}} \cdot \mathbf{H}_{\text{t}}, \tag{3}$$

where

$$\begin{aligned} \mathbf{H}_a &= \mathbf{H}_a(\theta_a, \varphi_a, f) \\ &= \hat{\theta}_a H_{a\theta}(\theta_a, \varphi_a, f) + \hat{\varphi}_a H_{a\varphi}(\theta_a, \varphi_a, f), \\ a &= \text{r } or \text{ t}, \end{aligned} \tag{4}$$

is a complex transfer function vector of the antenna relative to the isotropic antenna,

$$H_{\text{f}} = \frac{\lambda}{4\pi d} \exp(-\text{j}kd), \tag{5}$$

is the free space transfer function where

$$k = \frac{2\pi}{\lambda}, \tag{6}$$

is the propagation constant. The received waveform $v_{\text{r}}(t, d)$ can be found by using

$$v_{\text{r}}(t, d) = v_{\text{t}}(t) \otimes h_{\text{Friis}}(t, d), \tag{7}$$

where $v_{\text{t}}(t)$ is the transmitted signal waveform, $\otimes$ is the convolution operator, $h_{\text{Friis}}(t, d)$ is the impulse response of the extension of Friis' formula defined as:

$$h_{\text{Friis}}(t, d) = \mathcal{F}^{-1}\{H_{\text{Friis}}(f, d)\}, \tag{8}$$

where $\mathcal{F}^{-1}\{\cdot\}$ is the inverse Fourier transform.

3. Experimental Evaluation of Waveform Distortion for UWB-IR

The impulse radio signal that fully covers the FCC band 3.1 ~ 10.6 GHz [3]. The center frequency and the bandwidth were therefore set to be $f_0 = 6.85$ GHz and $f_{\text{b}} = 7.5$ GHz, respectively. The transmit waveform assumed in the simulation was a single ASK pulse with the carrier frequency f_0. To satisfy the bandwidth requirement of f_{b}, the pulse length was set to be $\frac{2}{f_{\text{b}}}$. Then the signal was band-limited by a Nyquist roll-off filter with roll-off factor $\alpha = 0$ (rectangular window) and passband $\left(f_0 - \frac{f_{\text{b}}}{2}, f_0 + \frac{f_{\text{b}}}{2}\right)$. The transmission process of the pulse waveform is simulated based on the measured transfer function of the antenna.

The vector network analyzer was operated in the response measurement mode from 3 GHz to 11 GHz, where port-1 was used as the transmitter port and port-2 was used as the receiver port, respectively. The measurement was done in an anechoic chamber to simulate free space. Both Tx and Rx antennas were fixed at the height of 1.72 m. We have chosen the biconical antenna for Tx and Rx antennas.

The largest dimension of each Tx and Rx antennas are the inclined height $D_t = D_r = 75$ mm. The largest dimension of the antenna considering the field regions are $D = D_t + D_r = 150$ mm. Then, 0.3 and 0.4 m TR separation distances are chosen for the Fresnel region, while 1.6 and 2.0 m TR separation distances are chosen for the far field region. The practical maximum measured distance, 4 m, is chosen as reference distance to estimate the accuracy of the antenna transfer function. The Tx and Rx antennas are assumed to be identical.

The rectangular density spectral waveform covering the FCC band, that is 3.1 GHz to 10.6 GHz is used to test the distortion of the received UWB waveform. This waveform is expressed by

$$v_t(t) = \frac{1}{f_{\max} - f_{\min}} [f_{\max}\text{sinc}(2f_{\max}t) - f_{\min}\text{sinc}(2f_{\min}t)], \tag{9}$$

where $f_{\min} = 3.1$ GHz is the minimum frequency, $f_{\max} = 10.6$ GHz is the maxmimum frequency and $\text{sinc}(x) = \sin(\pi x)/(\pi x)$.

4. Results and Discussion

The transfer function of Tx and Rx antennas are estimated by using the channel transfer function at 4 m, assuming that these antennas are with identical transfer function. Figures 1 and 2 show the magnitude of the transfer functions measured at 0.3 and 2.0 m distances. In Figs. 1 and 2, the measured values are compared with the predicted and complex form Friis' transmission formula. Both results are almost identical in the far field region, but the differences of magnitude are observed in the Fresnel region. We can clearly see that in the Fresnel region, the measured magnitude results are greater than the predicted magnitude results. This is due to the radial field in the Fresnel region. In the far field region, the radial field can be negligible.

Figures 3 and 4 the received UWB-IR, by using the measured transfer functions and those predicted by using the complex form Friis' transmission formula and the antenna transfer function. We can see a little difference between the measured and the predicted waveforms in the Fresnel region. In the far field region on the other hand, the received waveforms are almost the same. Figure 5 shows the path loss between two received UWB waveforms corresponding to the measured and the predicted transfer function at a distance of 0.3 m and 2 m. The path gain is more obvious in the Fresnel region. Figure 6 shows the correlation between two waveforms corresponding to the measured and the predicted transfer functions. It has higher distortion in the Fresnel region. While in the far field region, the distortion is very small.

5. Conclusion

This paper, computational of waveform distortion based on Friis' transmission formula in complex form has been experimentally studied to consider the UWB-IR transmission waveform. The error of the channel transfer function and path loss are observed in the Fresnel region caused by the radial field. More comprehensive studies are necessary to consider the type of antennas (size and current distribution) and to find how to compensate the error.

References

[1] H. T. Friis, "A Note on a Simple Transmission Formula," *Proc. IRE*, Vol 34, no 5, pp. 254-256, May 1946.

[2] J. Takada, S. Promwong and W. Hachitani, "Extension of Friis' Transmission Formula for UWB Systems," *IEICE Tech. Rep.*, May 2003.

[3] Federal Communications Commission, "Revision of Part 15 of the Commission's Rules Regarding Ultra-Wideband Transmission Systems," First Report and Order, FCC 02–48, Apr. 2002.

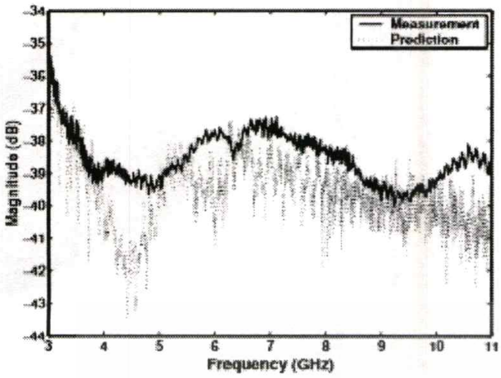

Figure 1: The channel transfer function at 0.3 m distances: magnitude.

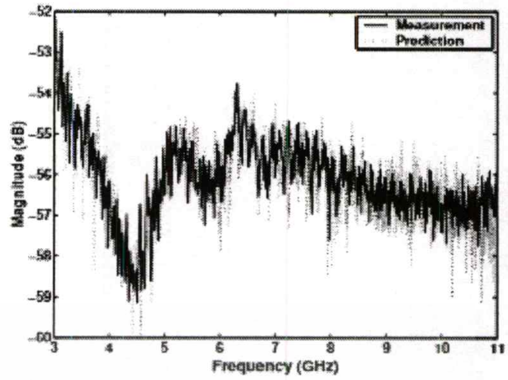

Figure 2: The channel transfer function at 2 m distances: magnitude.

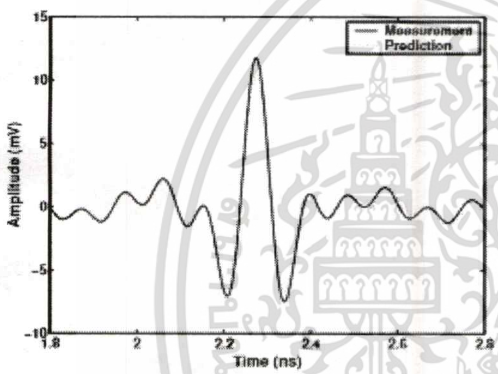

Figure 3: The received UWB waveforms at 0.3m distances.

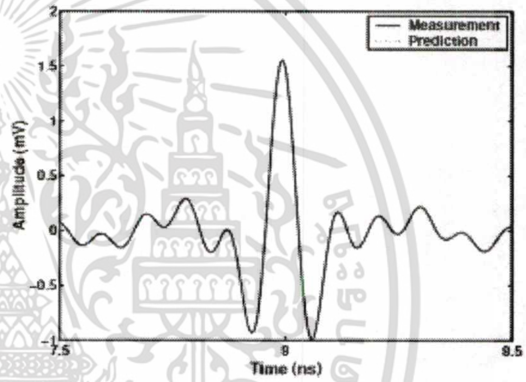

Figure 4: The received UWB waveforms at 2.0 m distances.

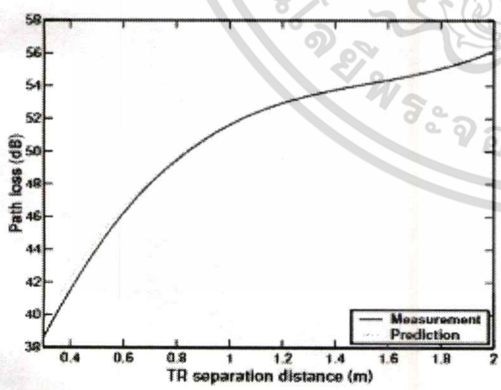

Figure 5: Path loss of the received UWB waveform.

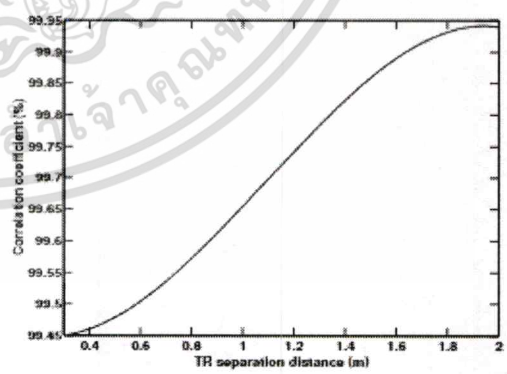

Figure 6: The correlation coefficient of the received UWB waveform.